Perspectives on Hypersonic Viscous and Nonequilibrium Flow Research

H. K. CHENG

Department of Aerospace Engineering
University of Southern California
Los Angeles, California 90089-1191

NASA/DOD Hypersonic Research and Training Program NAGW-1061
AFOSR Mathematics and Information Science Program 91-0104

PERSPECTIVES ON HYPERSONIC VISCOUS AND NONEQUILIBRIUM FLOW RESEARCH

H.K. Cheng
Department of Aerospace Engineering
University of Southern California
Los Angeles CA 90089-1191

FOREWORD

This report (USCAE 151) is based on a study prepared for the article "Perspectives on Hypersonic Viscous Flow Research" in the Annual Reviews of Fluid Mechanics. Owing to space limitation, the following material in §§6-8 was not included in the article that will appear. The original review study is documented here as a whole under a slightly revised title, reflecting an expanded scope to include aspects of nonequilibrium aerothermodynamics, combustion, and rarefied gas dynamics.

1. INTRODUCTION

The National Aerospace Plane (NASP) and several other space programs initiated during the past decade in the U.S. and abroad (see Williams 1986, Parks & Waldman 1990, Parkinson & Conchie 1990, Koelle 1990, Ito et al. 1990, Lozino-Lozinsky & Neiland 1989) have rekindled considerable interest in *hypersonics*. Almost one quarter of a century separates the present from the dynamical era of hypersonic flow research in the mid-1950s and early 1960s, during which critical flow physics problems posed by atmospheric reentry were identified and solved while many aspects of aerodynamic and aerothermodynamic theories were established. What, then, are the issues and advances in this field as perceived in the modern setting? The immense impact of the computer revolution on the design concept and analysis strategy, the experience with the Space-Transportation-System (Space Shuttle) program, as well as advances in material and propulsion technologies since the 1970s should all have made the modern research environment and progress vastly different from those of the Sputnik-Apollo era. This article examines issues and advances in current hypersonic flow research perceived to be of interest in theoretical fluid/gas dynamics. The scope and depth of the review are necessarily limited, as is the list of cited references, although the latter turns out to be quite extensive owing to the diverse nature of the field. Helpful are two recent texts by Anderson (1989) and Park (1990) which provide useful background material for the discussion of current issues. [See the reviews by Cheng (1990) and Treanor (1991).]

The nature of this diverse field may perhaps be appreciated by considering simplistically the flight Mach number M_∞ and the Reynolds number Re_∞ (or the Knudsen number $Kn = M_\infty/Re_\infty$) as two driving parameters which control the high-temperature real-gas properties and the molecular-transport processes. A lowering of Re_∞ (increasing Kn) as the vehicle ascends to the more rarefied atmosphere brings about *nonequilibrium* in the internal molecular excitations and flow chemistry, and in the translational motion of the particles as well. As with viscous and diffusive processes, they are controlled mainly by particle-collision events. The speed and altitude ranges of the Space Shuttle and the NASP ascent/descent corridors encompass most such nonequilibrium domains. Thus, apart from the fluid dynamic aspect of hypersonic viscous flows, one must address issues of nonequilibrium gas dynamics affecting the flows of interest, hence the use of "perspectives" in the article's title.

In the present framework, the study of viscous hypersonic flow will face transition problems of two kinds which represent, in fact, the two major areas of current research: the turbulence transition at the high Re range and, at the other end, the transition to the free-molecule limit. Work on fully developed turbulent boundary/shear layers are outside the scope of this review; some recent work applicable to turbulence transition in hypersonic boundary layers will nevertheless be noted. Readers may find helpful insight on turbulence modelling and CFD for aerodynamic flows offered in recent articles by Chapman (1992), Moin, (1992), Cheng (1989) and Mehta (1990). Towards the rarefied-gas regime, there are quite a few Direct Simulation Monte Carlo (DSMC) calculations of varying themes to be studied and several issues on continuum extension are in need of clarification. Works on gaseous radiation and scramjet combustion will be cited only in relation to nonequilibrium gas dynamics and CFD studies. A recent article by Tirsky (1993) on hypersonic flow research is called to author's attention. The work presents a perspective quite different from this review and may otherwise be considered complementary to the material discussed in §§6 - 8 below.

2. HYPERSONIC AIRCRAFT AS WAVERIDER

On hypersonic vehicle design and research, Townend (1991) lists three recurrent themes: 1.

replacement of expendable ballistic space launchers with reusable aerospace planes, 2. hypersonic airlines, and 3. transatmospheric orbital transfer vehicles. Central to all three is research which aims at integrating air-breathing propulsion into an aerodynamic design called the "waverider". This term refers to a concept evolved from Nonweiler's (1963,1990) study which utilized the streamlines behind a known shock *wave* for generating examples of three-dimensional (3-D) lifting bodies in a supersonic flow--a particular example of which is the caret wing generated from streamlines behind a plane shock (see Küchemann 1978, pp. 74-79, 450-514; Stollery 1990).

2.1 Waverider as a Generic Design; The Breguet Range

A great number of recent studies and overviews on waveriders were presented in the proceedings of an international waverider symposium (Anderson et al. 1990), where substantial improvement in lift-to-drag ratio (L/D) and other aerodynamic features over standard configurations are reported. The article by Eggers et al. (1990) extensively reviews the aerodynamic design development related to the waverider concept and is itself a valuable document in hypersonic aerodynamics. At this juncture, it will be refreshing to recall a discussion by Küchemann on aircraft cruising range and his vision of hypersonic flight.

Küchemann (1978, pp. 7-9) anticipated a trend of increasing propulsive efficiency η_p with flight speed, and a corresponding decreasing trend in the lift-to-drag ratio of waverider aircraft, so that the product $\eta_p L/D$ remains roughly constant--being close to the value π. With this, and the provision that the fuel carried is not too small a fraction of the all-up weight, Küchemann concluded from the Breguet range formula that a nonstop flight to the farthest point on the globe is feasible even if hydrocarbon fuel is used, *irrespective* of flight speed. For a Mach-8 Orient Express or the NASP X-30 at a comparable speed, the cruise would take about *two* hours. This conclusion is made explicit in Küchemann's (1978, p.551) "spectrum of aircraft" reproduced here in Fig. 1. It shows the maximum ranges of four types of aircrafts designed for cruising at four very different Mach numbers, each allowing a two-hour flight time.

2.2 Waverider Wing Studies

THE VISCOUS CORRECTIONS Skin friction must be included in the performance analysis of a waverider wing. Results of optimization which takes into account skin friction have been referred to as "viscous optimized" (Bowcutt et al. 1987, Corda et al. 1988). The viscous optimized waveriders obtained are seen to differ considerably in shape depending on (turbulence) transition locations *assumed* in the calculations, signifying the critical need of a reliable transition prediction method (§5).

BOUNDARY-LAYER DISPLACEMENT, FLOW CHEMISTRY AND HIGH-ALTITUDE EFFECTS Owing to the boundary-layer displacement effect at sufficiently low Reynolds numbers, wing loading, skin friction and surface heating rate may increase significantly for a thin wing at low incidence. Anderson et al. (1992) studied examples of waveriders with a 60-meter chord optimized for this viscous-interaction (displacement) effect. The displacement effects on lift and drag are affected little by the optimization performed in the study, which nevertheless, alter the waverider planform and its thickness distribution drastically. This observation signifies a configuration *insensitivity* at a given Re and M_∞, which could be translated to a greater degree of freedom for the designers. The effect of air chemistry on waverider aerodynamics has also been studied (Anderson et al. 1992) but found to be small for the examples considered.

For higher altitude applications, Anderson et al. (1991) studied waverider wings 5-meter in length at altitudes of 80-120 km, corresponding to a Knudsen-number range from 10^{-3} to a unit order, even though the wing was generated by an *inviscid* procedure. In their study, Potter's (1988)

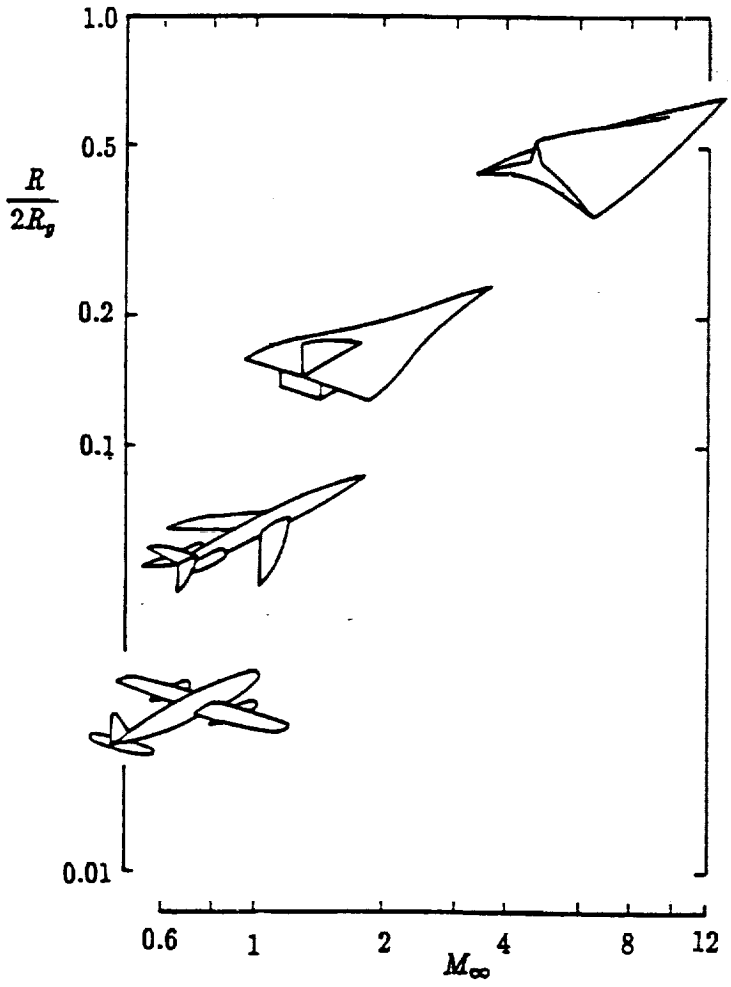

Fig. 1 The Spectrum of Aircraft (from Küchemann 1978): Range covered by a two-hour flight as a function of cruise Mach number for four different aerodynamic designs. The value $R/2R_g = 0.5$ represents the distance to the farthest end of a great circle route.

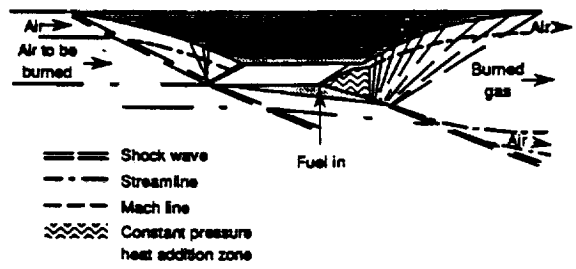

Fig. 2 Schematic of a hypersonic ramjet (from Billig 1992).

bridging function for empirical correlation of rarefied hypersonic-flow data was considered (also see Warr 1979, Wilhite et al. 1985). This and other questions may better be discussed in the context of low-density hypersonic flows in §8.

ISSUES WITH A SHARP LEADING EDGE A question on the practicality of the waverider design arises, which concerns the *sharp* leading edge inherent to the inviscid solution procedure used. An important issue was raised by Nonweiler, namely, whether a genuinely sharp leading edge made of available materials can survive the heat flux from hypersonic flight without the aid of active cooling. An answer was offered by the "conducting plate" theory and experiment (Nonweiler et al. 1971, Nonweiler 1990) which show that solid-body conductivity and radiative cooling can together be effective in limiting the temperature on a sharp-edged wing. For a 14° wedge-shaped leading edge built from material with conductivity comparable to graphite, the maximum temperature on a 75° swept wing at a speed of 6.5 km/sec is not expected to exceed 2000°K, according to the study. Recent progress in material research (e.g. Sanzero 1990) could make this passive-cooling approach more attractive. A thin/slender configuration with or without a sharp leading edge is apparently preferred over a nonslender/blunt shape in the quest for a high L/D. This may be essential for the cruise economy as well as cross range capability in a transatmospheric operation (Walberg 1985).

2.3 Integrated Aerodynamic Design

The merit of a waverider or any aerodynamic design cannot be assessed without considering the constraints placed by the power plant installation, propulsion concept and other details in an integrated design, (Küchemann 1978, Townend 1991). Figure 2 indicates the various parts of the external and internal flows of a scramjet engine of a generic design and the need for an integrated analysis (Billig 1992). The surface pressure on the ramp would add substantially to the total lift L and drag D; the rear portion where the burned gas exits takes the form of a "half nozzle" where the thrust T is principally derived, and the pressure also contributes to the lift and pitching moment. As an integrated system, one may speak of the net thrust (T-D) available for acceleration. As the scramjet vehicle ascends to higher altitudes, the ability to accelerate further depends on the precarious balance between the diminishing T and D.

3. VISCOUS INTERACTION: COMPUTATIONAL METHODS

The fluid dynamics of hypersonic flows is complicated by the interaction of the boundary layer and shear layer with shock waves, leading to flow separation and instability not amenable to straightforward analyses. The need for numerical solutions to the Navier-Stokes (NS) or other full equation systems has been made apparent in Fig. 2, where significant interaction of boundary layers with shock/expansion waves occurs in most regions. Note that in the straight precombustion passage (called "isolator") in Fig. 2, a shock train (not shown) must form through wave reflection and viscous interaction. Complicated shock-shock interaction patterns can create a supersonic jet impinging on the cowl lip, causing an unexpectedly high local heating rate as was first investigated by Edney (1968) and later by Holden et al. (1988) and Glass et al. (1989); this has yet to be explained by a viscous interaction analyses (cf. Fig. 3 reproduced from Weiting 1990). As a prelude to the discussions of the following sections, several major approaches to viscous-flow calculations underlying much of the current hypersonic flow studies will be noted; their extension to nonequilibrium flow calculations will be discussed in specific applications later in §6. Some of the basic computational procedures for compressible viscous flow calculations have been elucidated in texts and monographs (e.g., Anderson et al. 1984, Hoffman 1989). The CFD approaches of interest here will be discussed in three categories according to the level of approximation for the governing equations.

3.1 Interacting Boundary Layer Equations

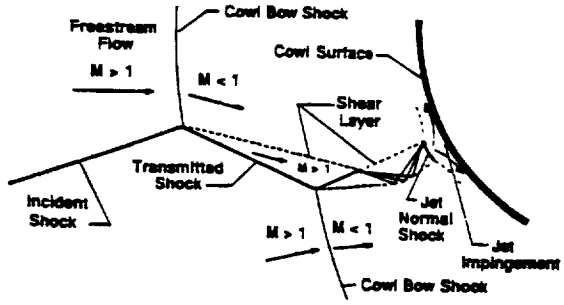

Fig. 3 Interaction of incident shock and bow shock near engine cowl leading edge: Edney's Type IV supersonic jet interference pattern (sketch reproduced from Weiting 1990).

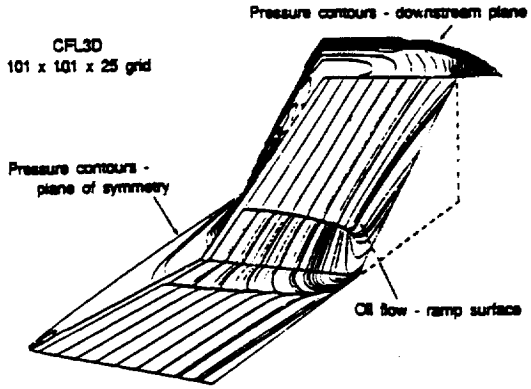

Fig. 4 Surface oil flow pattern and pressure contours in the symmetry plane and downstream plane computed by a thin-layer NS code (CFL3D) for a ramp on flat plate at $M_1 \sim 14$, $Re \sim 10^5$ (Rudy et al 1991). The analysis resolved discrepancies between experiment and earlier 2-D calculations.

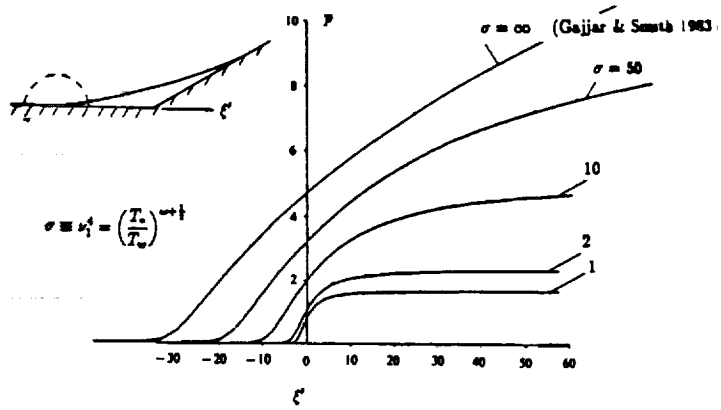

Fig. 5 Normalized over pressure in a compressive free-interaction for
$\sigma \equiv (T_*/T_\omega)^{\omega+\frac{1}{2}} = 1, 2, 10, 50, \infty$ (Brown et al 1990). Note the plateau pressure depends on surface temperature, Mach and Reynolds numbers through σ and T_* defined in the text.

Unlike in standard boundary layer theory, the streamwise pressure gradients in the boundary-layer equations are not given a priori and are determined in a system coupled to the Euler equations governing the outer flows. The steady-state version of the equations allows upstream influence and flow separation and is comparable to a composite form of the PDEs in triple-deck theory (e.g., Werle & Vasta 1974; Burggraf et al. 1979; also Anderson et al. 1984).

3.2 Parabolized Navier-Stokes (PNS)

Even if the viscous interaction is strong, the thin viscous layer permits the deletion of most streamwise partial derivative terms in the viscous, heat-conducting, and diffusive parts of the NS equations. For steady-state applications, the reduced nonlinear equations give the appearance of PDEs of parabolic type, hence the name PNS. With a hypersonic free stream, the upstream influence can be omitted in the less viscous part of the external flow, and the PNS system may then be integrated simply as an initial boundary-value problem by marching in the downstream direction. Documented results show excellent capability of the methods in shock-capturing, and in describing the interactions on the global scale as well as capturing cross-flow separations. As methods for analyzing viscous interaction, however, a short coming of these marching procedures is their preclusion of the upstream influence of the downstream condition and reverse flows owing to the special treatments of the streamwise pressure term needed to suppress the *departure solution* (Vigneron et al. 1978; Anderson et al. 1984, pp. 433-440; for recent PNS implementation in hypersonic flow, see Butta et al. 1990; Tannehill et al. 1990; Krawczyk et al. 1989).

In passing, one notes that the equations in viscous shock-layer theories (Davis 1970, Moss 1976, Cheng 1963; also Gupta et al. 1992) may also be regarded as the simpler versions of the PNS using shock fitting. They may best be discussed in the context of the continuum extension to the rarefied gas dynamic regime in §8, inasmuch as a considerable number of their applications have been made during the last decade in studies comparing the continuum and particle-simulation models (Moss et al. 1987, Moss & Bird 1985, Cheng et al. 1989,1990,1991).

3.3. Iterative/Time-Accurate Navier-Stokes

THIN-LAYER NAVIER-STOKES To retain the upstream-influence capability, one may restore the time-dependent terms to the PNS equations, solving them as a *time marching*, initial boundary-value problem, or apply an *iterative* procedure to the (steady) PNS equations with suitable outflow boundary conditions. This version is often referred to as the *thin-layer* NS and is believed to be basic to several codes in current use: ARC3D (Pulliam & Steger 1980), F3D (Ying et al. 1986), NS3D (Blottner 1990), and also CFL3D (Vasta et al. 1989). A space-marching iterative procedure called the "supra-characteristic method" (Stookesberry & Tannehill 1986) also belongs to this class. In the first two codes, flux-vector splitting with upwind differencing (Steger & Warming 1980; van Leer 1982) or similar techniques are used, these prove to be robust in many shock-capturing calculations (Roe 1986, van Leer et al. 1987). The F3D code has been further developed and used successfully in 3-D hypersonic flow analyses (Ryan et al. 1990), nonequilibrium hydrogen-air reaction (Lee & Deiwert 1990) and the hypersonic flow through an expansion slot in a 3-D ramp (Hung & Barth 1990). TVD (Total Variation Diminishing) and similar schemes were used in many of these works to enhance the shock-capturing capability (cf. Yee 1987). Compared to the full NS calculations, the thin-layer version may represent a considerable saving in computer resources and programming effort; global convergence to the steady state can be accelerated with some zonal strategy, as seen from the cited examples.

FULL NAVIER-STOKES CALCULATIONS Similar remarks apply to the full NS equations and calculations. Among the full 3-D NS codes used in current hypersonic flow analyses is the LAURA (Langley Aerothermodynamic Upwind Relaxation Algorithm) designed for finite-volume formulation (see

Gnoffo 1989); LAURA adapts Roe's averaging to flux components across cell boundaries for the convective terms (see Roe 1986) and Harten's (1983) symmetric TVD scheme (see also Yee 1987). Unique in this relaxation procedure is the *point-implicit* strategy, which is believed to render the procedure stable for an arbitrary Courant number without the need of solving large, block-tridiagonal matrix equations. The LAURA code has been applied to a variety of nonequilibrium aerothermodynamic problems as well as rarefied, hypersonic flow studies (cf. Gnoffo 1990, Greendyke et al. 1992), to which we shall return later for comments.

The procedure of MacCormack's explicit, time-split, predictor-corrector method (MacCormack & Baldwin 1975, Hung & MacCormack 1975) and the implicit version (MacCormack 1982) solve equations in finite-volume conservation-law form and are supposedly second-order accurate in space and time, as elucidated in the text of Anderson et al. (1984). Application of the explicit 2-D version by Hung & MacCormack (1975) to flow past a flat plate with a compression corner at $M_\infty = 14.1$, $Re_\infty = 1.04 \times 10^5$, agree quite well with experimentally measured surface pressure, heating rate, and skin friction (Holden & Moselle 1969) for ramp angles $\alpha = 0$-$18°$. The same set of experimental data was also compared with solutions by the supra-characteristics method in Stookesberry & Tannehill (1986). However, the comparison for $\alpha = 24°$ was not satisfactory in either study for the reason be noted shortly. A 3-D version of a similar procedure was successfully applied to a complete reentry configuration at Mach 6 by Shang & Scherr (1986), assuming $\gamma = 1.40$ and a Baldwin-Lomax (1978) turbulence model (cf. Anderson 1989, pp. 353-359). In the implicit version, a stage is added to each of the predictor and corrector steps, where an approximately factorized time-dependent operator is applied to implicitly update the unknowns by simply inverting bidiagonal matrices as was done in the explicit version. Whereas the procedure is unconditionally stable for unbounded time steps Δt according to linear model analyses, the products $\mu\Delta t/\varrho(\Delta x)^2$ and $\mu\Delta t/\varrho(\Delta y)^2$ are required to be bounded to maintain accuracy. One observes, however, that the latter requirements are similar to, and almost as restrictive as, the stability condition for an explicit method applied to a diffusion/heat equation, and that the density ϱ in these products can cause severe problems in rarefied hypersonic flow applications.

The second-order accurate, compressible NS solver recently proposed by MacCormack & Candler (1989) is virtually a *relaxation* procedure and appears to be extremely promising for 3-D applications, according to MacCormack (1990). Type-dependent procedures have been effectively implemented according to the flux-vector splitting algorithm in solving equations in conservation-law form (Steger & Warming 1980). The *splitting*, applied mainly to the streamwise flux, is believed to help relaxation convergence by virtue of the increased weight of the diagonal elements in the block tridiagonal matrix of the difference equations. In MacCormack & Candler's (1989) procedure, the Gauss-Seidel line relaxation is adopted to solve the *unfactored* matrix equations, thereby avoiding unwarranted errors from the approximate factorization, which slows down convergence. The new procedure allows large time steps, and the calculation can be performed on a common work station. It is unclear if convergence acceleration routines (e.g. Cheung et al. 1991) would be helpful in further enhancing the method's performance. Recently, this procedure has been adapted to solve the (full) Burnett (1936) equations for rarefied hypersonic flows (Zhong et al. 1991 a,b), for which issues with boundary conditions and solution uniqueness remain unresolved (see §§8.5, 8.6 below).

IMPORTANCE OF 3-D INFLUENCE We return now to the comparison of Hung & MacCormack's (1975) calculation with Holden & Mosselle's (1969) measurement for the case with the ramp angle $\alpha = 24°$ mentioned earlier. In this case, Rudy et al. (1991) used the thin-layer CFL 3D (Vasta et al. 1989) code to demonstrate that spanwise (global) 3-D effects can resolve all the noticeable discrepancies. The computed surface oil flow and pressure contours in the symmetry plane and a downstream plane are reproduced in Fig. 4. This provides perhaps an excellent example in which 3-D computation has proven crucial in settling a fluid dynamic issue which would have been perceived as being 2-D in

origin. Among other computer programs currently being used in viscous hypersonic flow study are those of Edwards & Flores (1990), Thomas & Neier (1990), and Liu & Jameson (1992).

4. VISCOUS INTERACTION: THEORETICAL DEVELOPMENT

We turn next to the development of viscous interaction theory in this section and later to the investigation of the related instability problem of hypersonic boundary layers in §5.

4.1 Viscous Interaction on the Triple-Deck Scales

Significant *global* interaction of a laminar boundary layer with an external hypersonic flow ($M_1>>1$) has been the subject of extensive investigation in the past (e.g. Hayes & Probstein 1959, Moore 1964, Cox & Crabtree 1965, and the review by Mikhailov et al. 1971). There is yet another more universal and important interactive feature of a boundary layer occurring on a much *shorter* scale noted earlier by Lighthill (1953), which permits upstream influence and separation and became the focus of a vast number of theoretical studies two decades later (see reviews by Stewartson 1974, 1981; Smith 1982, 1986; Sychev 1987). Central to all the recent work is the triple-deck theory which stipulates a *three-tier* stucture made up of *lower*, *main* and *upper* decks, with the streamwise scale short enough that a small self-induced pressure rise is sufficient to provoke flow reversal and separation.

4.2 Triple-Deck Theory Applied to Hypersonic Flow

The basic parameter controlling the triple-deck structure for a *locally supersonic* external flow can be written for the present purpose as (Stewartson 1974)

$$\epsilon \equiv \Gamma(\frac{\gamma-1}{2})\frac{M_1}{\sqrt{\gamma(M_1^2-1)}}\left(M_1^3\sqrt{\frac{C}{Re_1}}\right)^{1/4} \tag{4.1}$$

where Γ is a function of wall temperature and wall shear immediately upstream of the interaction zone, and the product inside the large bracket is simply the Lees-Stewartson global-interaction parameter

$$\chi \equiv M_1^3\sqrt{\frac{C}{Re_1}} \tag{4.2}$$

familiar from the classical theory. In the preceding, the subscript "1" refers to the condition immediately upstream of the triple deck and the constant C is the Chapman-Rubesin coefficient μ_*T_1/μ_1T_*, where the asterisks refer to the reference temperature of the hypersonic boundary layer. It is apparent from (4.1) that χ remains to be the important parameter controlling the viscous interaction on *both* global and triple-deck scales. Characterizing the theory for this flow structure are the orders of magnitudes of the thickness ratios of the lower, the main and the upper decks, and also the normalized pressure and streamwise-velocity perturbations, which are representable, respectively, as

$$\epsilon^5,\ \epsilon^4,\ \epsilon^3,\ \epsilon^2\ \epsilon \tag{4.3}$$

(The streamwise length scale Δ for the triple deck is the same as that of the upper deck.) This version of the theory is to be referred to as the *standard* version and requires the ϵ in (4.1) to be asymptotically small, and is clearly inapplicable to a regime where χ is not small. There is however a Newtonian version of this approach which considers $(\gamma-1)/2$ being asymptotically small in addition

to M_1 being large, while allowing an unbounded χ (§4.4). The upstream influence through the lower deck may be best seen from the formulation of Rizzetta et al. (1978) using the shear $\tau \equiv \partial u/\partial y$ as a dependent variable, in which a Neumann boundary condition for τ at the wall (y = 0), after eliminating the pressure gradient, is

$$\frac{\partial \tau}{\partial y} = \frac{d^2}{dx^2} \int_0^\infty (\tau - 1) dy \tag{4.4}$$

where the second x-derivative makes the *elliptic* nature of the problem apparent.

Among the examples (see Stewartson 1974; Smith 1982,1986) is the *free-interaction* solution which is an eigen/departure solution that is admissible if provoked. The latter leads to separation and flow reversal in the lower deck, and reaches a pressure plateau downstream; it represents physically the precursor at the head of a large recirculation region. For a ramp angle in a suitably small range, solutions with recirculation and reattachment on the ramp downstream were obtained by Rizzeta et al. (1978).

4.3 Is Departure Solution Admissible at Large χ?

The foregoing discussion would suggest that departure solutions of the triple-deck theory are unlikely at large χ (strong global interaction). A classical example of global interaction at an unbounded χ is that of an aligned flat plate, for which the self-similar solution at a uniform wall temperature yields a self-induced pressure p/p_∞ proportional to χ (Stewartson 1955, Hayes & Probstein 1959). Neiland (1970) found, however, that an indeterminancy exists for an expansion of this solution in descending powers of χ, i.e.,

$$\frac{p}{p_\infty} = D_\infty \chi [1 + \cdots + a_1 \chi^{-2n} + \cdots] \tag{4.5}$$

where for a certain exponent n, the constant a_1 cannot be determined. The finding suggests an upstream influence excluded by the solution procedure. Using a tangent-wedge pressure formula, and assuming a unit Prandtl number and an insulated wall, Neiland found n = 50.6. This value was confirmed subsequently in the analysis of Werle's et al. (1973) analysis which considers a wide range of wall temperature, and in Brown & Stewartson's (1975) investigation where the eigen solution was found to be insensitive to the approximation made on the outer flow. There, the exponent n was shown to be a function of the specific-heat ratio γ and of the wall-to-stagnation temperature ratio. These features may nevertheless be reconciled with the triple-deck formalism discussed below.

4.4 The Theory for $\gamma \to 1$

The impasse in the triple-deck theory posed by large χ is overcome by the theory of Brown et al. (1975) based on small $(\gamma-1)/2$ and high M_1^2, which could be called a Newtonian theory (Hayes & Probstein 1959) but which is less restrictive than the latter since the assumption of a strong shock is not strictly required. Let ε, ε_p and Δ gauge the orders of magnitude of the velocity and pressure perturbations, and the streamwise length scale of the triple deck, respectively. These can be expressed in this case for a nonvanishing χ explicitly as

$$\varepsilon = (\gamma-1)(T_w/T_o)^2 C\chi^{-1/2}, \quad \varepsilon = (\gamma-1)(T_w/T_o)^6, \quad \Delta = (\gamma-1)^3(T_w/T_o)^6, \tag{4.6}$$

showing that a triple-deck structure is possible for $\gamma \to 1$. They also suggest that wall cooling should make the theory much more accurate. Using the tangent-wedge approximation, the crucial pressure-displacement relation in Brown et al. (1975) needed for closure of the interaction problem can be

written as

$$\mu p = \frac{d}{d\xi'}(A + p) \tag{4.7}$$

where A is a displacement due to the lower deck, and μ is a constant of the order $(\gamma-1)(T_w/T_o)^6\chi^2$ in the case of small χ. This may be compared with p = -dA/dx in the (standard) supersonic triple deck theory. Computational studies with this version of the theory have been made for a compressive ramp (Rizzetta et al. 1978) and for free interaction (Gajjar & Smith 1983).

On the other hand, for finite χ and small $(\gamma - 1)/2$, (4.7) leads to

$$0 \approx \frac{d}{d\xi'}(A + p) \tag{4.8}$$

which implies that the boundary-layer outer edge, hence the flow in the upper deck, is little affected by the interaction. In this connection, one may examine whether the triple-deck result can be reconciled with Nieland's algebraic eigensolution (4.5). The latter may now be interpreted as

$$a_1\chi^{-2n} = b_1\left(\frac{\chi}{\chi_1}\right)^n \sim b_1 \exp.\left(n\,\frac{\chi-\chi_1}{\chi_1}\right) \tag{4.9}$$

Note that $\chi \propto x^{-1/2}$ and that the triple deck is centered at x_1. Now the free-interaction solution in the theory of Brown's et al. (1975) gives a pressure precursor of the same form as (4.9) with the exponent n being identified as $n = (0.8273)/\Delta = O[(\gamma-1)^{-3}(T_w/T_o)^{-6}]$, which is indeed a large number for the γ and T_w/T_o of interest, as was anticipated. The Newtonian version of the analysis (Brown et al. 1975) remains to be completed with the inclusion of the centrifugal correction in the Busemann pressure formula; this is expected to alter substantially the pressure-displacement relation (4.7).

4.5 Critical Influence of Wall Cooling

For hypersonic flight applications, theory and analysis must take into consideration the effect of a low wall-to-stagnation temperature ($T_w/T_0 \ll 1$). It may be noted that the assumption $T_w/T_o = O(1)$ is implicit in the standard theory, and the wall temperature need not fall too far below the stagnation/recovery level before a significant departure from the standard theory can occur, as the following will confirm.

The analysis of Brown's et al. (1990) on the triple deck for small χ identifies a critical wall temperature level T_w^*:

$$s_w^* \equiv \frac{T_w^*}{T_o} \sim \left[\lambda^5\gamma^{-1/2}\left(\frac{2}{\gamma-1}\right)^2\chi_1\right]^{\frac{1}{4\omega+3}} \tag{4.10}$$

where λ is a normalized undisturbed wall shear (equal to 0.332 for an aligned flat plate), and ω is the exponent in the viscosity-temperature relation $\mu \propto T^\omega$; the Newtonian factor $2/(\gamma-1)$ is included to indicate its influence but the limit $\gamma \to 1$ was <u>not</u> taken. Depending on the ratio T_w/T_w^*, three distinct wall-temperature ranges exist:

$$\text{(i) Supercritical: } T_w \gg T_w^*, \text{ (ii) Transcritical: } T_w = O(T_w^*), \text{ (iii) Subcritical: } T_w \ll T_w^* \tag{4.11}$$

For the supercritical and transcritical ranges, the set of scale factors ε, ε_p and Δ is not basically different from that of the standard theory

$$\varepsilon = \lambda^{-2}\frac{\gamma-1}{2}s_w^{2\omega}\nu_1, \quad \varepsilon_p = \lambda^{-2}\frac{\gamma-1}{2}s_w^{2\omega+1}\nu_1^2, \quad \Delta = \lambda^{-5}\gamma\left(\frac{\gamma-1}{2}\right)^3 s_w^{4\omega+2}\nu_1^3, \tag{4.12}$$

where

$$s_w = \frac{T_w}{T_o}, \quad \nu_1 \equiv \left(\frac{s_w^*}{s_w}\right)^{\omega+\frac{1}{2}}. \tag{4.13}$$

The relation between the pressure rise and the lower-deck displacement for the ranges (i) and (ii) can be reduced to

$$P_1 = -\frac{d}{d\xi'}(A + \nu P_1) \tag{4.14}$$

where $\nu = k\nu_1$, and k is a constant of order unity determined by the boundary-layer profiles just upstream of the triple deck, independent of χ_1. The term νP_1 in (4.14) is absent from the standard theory, and represents a *transcritical* (cold-wall) effect. For the subcritical range ($s_w \leq s_w^*$), the gauging parameters of (4.12) must change in order to remain small, to keep the reduced PDE in canonical form and to avoid degeneracy in the P-A relation. This is accomplished simply by replacing ν_1 therein by 1/k, and (4.14) changes over for the subcritical case to

$$\frac{d}{d\xi'}(P_1 + A) = -\nu_1^{-4} P_1 \tag{4.15}$$

Interestingly, the relative scales of the triple deck, i.e. ε and Δ, no longer depend on the Reynolds and Mach numbers in this case and vanish with s_w.

Figure 5 reproduces the results of Brown et al. (1990) for the overpressure in a free interaction for $\sigma \equiv \nu_1^4$ in the range of $1 < \sigma < \infty$, with the origin of ξ' located at the separation point. The existence of the transcritical and subcritical s_w-ranges was anticipated in Neiland (1990, private communication), the length scales therein differ however from those in Brown et al. (1990). The analysis of Brown et al. shows clearly the drastic reduction in the triple-deck length scales hence in the extent of the upstream influence as s_w vanishes. This means that laminar separation can occur but becomes more abrupt under a strong cooling.

5. BOUNDARY-LAYER INSTABILITY AND TRANSITION STUDIES

Many investigations of flow instability and turbulence transition in hypersonic boundary layers have been undertaken recently. The development is helped substantially, perhaps, by the sequence of analyses on *compressible* boundary-layer instability made decades earlier by Mack and others (see reviews by Mack 1984,1987a,b; Roshotko 1976).

Some caution should be exercised at this juncture on the use of the viscosity-temperature (μ-T) relation in extending the stability analysis to high-temperature real-gas flow, apart from other more obvious considerations. According to a recent study (Kang & Kunc 1991), for example, the viscosity of dissociating iodine at T = 1000-2000°K will have a *negative* slope in the μ-T relation, i.e. $d\mu/dT<0$; similar properties may occur in other dissociating/ionizing gases and their impact on the stability analysis need to be ascertained. The other aspect in need of caution is the assumption of translational equilibrium in certain stability and transition calculations, where the combination of low Re and high M_1 makes the gas-rarefaction effect important. Take for example, a hypersonic boundary layer on a slender/thin body, which may have a boundary-layer thickness δ of 2% the global scale L, or larger; in this case, it can be shown that the local mean free path is of the of δ.

5.1 Parallel-Flow Instability Applied to Compressible Boundary Layers

Lees & Lin (1946) extended the viscous (Tollmien-Schlichting waves) and inviscid (Rayleigh theorem) results of parallel-flow instability to the compressible case. They noted that the condition $D(\varrho DU) = 0$ (with $D \equiv d/dy$) signifies a maximum angular momentum and plays the same role in compressible theory as does $D^2U = 0$ (an inflection point) in incompressible theory. Unlike in the incompressible case, this generalized inflection point can be found at some $U = U_s$ in the compressible boundary layer on a flat plate, and therefore neutrally stable waves with phase velocity $c = U_s$ can

exist. Lees & Lin limited their consideration to 2-D subsonic relative waves, i.e. $|U(y)-c|<a(y)$. This rules out the "supersonic relative waves" with $|U(y)-c|>a(y)$ and the possibility that, in a supersonic boundary layer, the TS-type waves are most amplified at some oblique (wave) angles. Allowance of supersonic relative waves would render possible acoustic wave propagation and reflection within the boundary layer, admitting a sequence of *higher modes* for each phase velocity, as Mack (1984,1987a,b) subsequently found. [The modes are designated/ordered by a number "n" according to the sign changes (zero crossings) occurring in the pressure profile.] The second mode turns out to be the most unstable for flat plates and slender cones at high Re (inviscid) and also for all Re (viscous) at $M_1>4$, as was confirmed by subsequent experiments (discussed below). The neutral stability waves, both *inflectional* and *noninflectional*, are significant (as they are in classical theory) in that they identify with parts of the boundaries delimiting the instability/stability domains of interest. Figures 6,7 (reproduced from Mack 1985) present these curves of *neutral* instability in the domain of wave number α and Mach number M_1 for 2-D inflectional and noninflectional waves, respectively. The calculations were made for an insulated flat plate. Note that a sequence of noninflectional waves of *neutral* stability can exist for each c in the entire range $U_1 \le c \le U_1 + a_1$, but the results for $c = U_1$ shown in Fig. 6 are more important since each curve therein forms a part of the boundary for some genuinely unstable domain.

Among several peculiar features of Figs. 6,7 are the similarity of the two graphs in trends at high and low α, and the drastic slope change together with what appears to be a mode-switching behavior in Fig. 6, to be delineated in §5.3 below. One unique feature of a boundary layer with high M_1 is the progressive movement of the generalized inflection point towards the boundary-layer outer edge as M_1 increases. Thus at high M_1, this location falls inside the "edge layer" (Bush & Cross 1967, Lee & Cheng 1969) and the stability analysis must take into consideration the appropriate μ-T law. An adverse effect of wall cooling must be noted. At $M_1 = 10$, Mack's (1985) calculations revealed that the temporal amplification rates of the second, third and fourth modes at $T_w/T_o \sim 0.05$ are almost twice the corresponding rates for an insulated wall. This was confirmed experimentally at least for the second mode.

5.2 Experimental Studies of Hypersonic Boundary Layer Transition

There have been primarily three sets of experimental studies on hypersonic boundary layer instabilities at $M_1 = 4.5$-8.5 reported in Kendall (1975), Demetriades (1978) and Stetson et al. (1988). These focused on flat plates and cones in wind tunnels and employed hot-wire anemometer techniques. Kendall's experiments confirmed the existence of the second mode and its dominance in a hypersonic boundary layer, Demetriades verified Mack's findings on the adverse wall cooling effect on the second mode, and Stetson et al. investigated tip-bluntness, wall cooling, and other effects on slender cones. The latter studies and related works are comprehensively reviewed in Stetson & Kimmel (1992) who also noted the existence of a harmonic of the second mode unaccounted for by the theory. Figure 8, reproduced in part from Malik et al. (1990) shows good agreement of Stetson's cone data at $M_\infty = 8$ with Mack's calculation for the corresponding outer-edge Mach number $M_1 = 6.8$ in the second-mode frequencies near the maximum growth rate. The noticeable difference in the magnitude of the peak growth rate was believed to be caused by the inadequate accuracy of the mean flow represented by the boundary-layer solution, but the results based on the PNS generated mean flow in the study of Malik et al. (1990) were still far from the mark (cf. dashes and dash-dots in Fig. 8). However, a more recent analysis by Simen & Dallmann (1992) produces growth rates (reproduced in dots) rather close to the measurements near the peak, attributed principally to the merit of a version of thin-layer NS used in the mean-flow analysis.

5.3 Asymptotic Properties at High M_1

NEAR-MODE CROSSING Mack's result shown in Fig. 6 indicates the existence of a *segment* on the

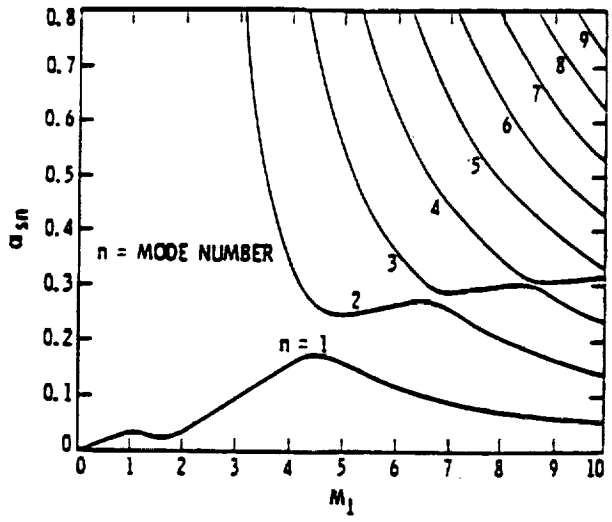

Fig. 6 Wave number as function of outer-edge Mach number of the neutral *inflectional* instability modes admissible to the inviscid stability equations of a compressible boundary layer on an aligned flat plate (from Mack 1984).

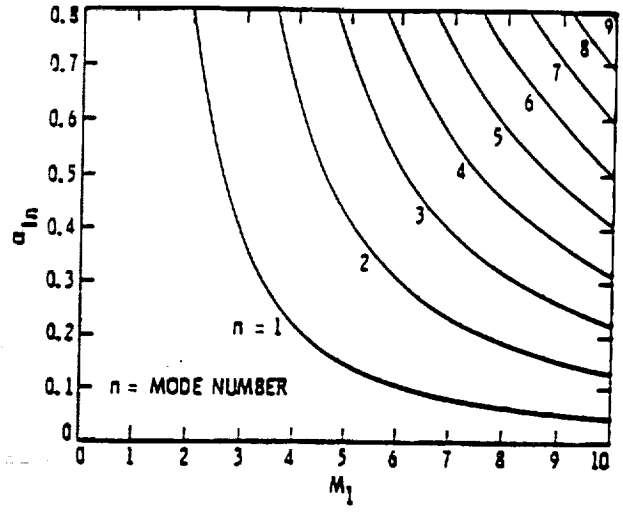

Fig. 7 Wave number as function of outer-edge Mach number of the neutral *non-inflectional* instability modes admissible to the inviscid stability equations of a compressible boundary layer on an aligned flat plate (from Mack 1984).

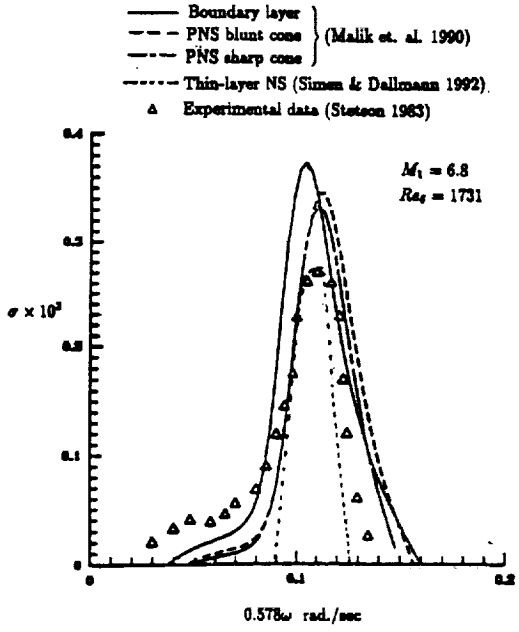

Fig. 8 Comparison of amplification rates of the second mode as function of frequency using four different basic-state equations with experimental data for boundary layer on a cone at $M_1 = 6.8$, $Re_\delta = 1731$ (Results and data from Malik et al 1990, Simen & Dallman 1992, Stetson 1983).

neutral curve of *each* (inflectional) mode where the slope $d\alpha/dM_1$ becomes positive, while the slopes are negative elsewhere and on the noninflectional neutral curves in Fig. 7. This segment has been alluded to as the "vorticity mode" (cf. Mack 1984), which will be named hereafter the *vorticity submode* (of each inflectional neutral mode). The parts on the neutral inflectional curves with negative $d\alpha/dM_1$ will be called acoustic submode and those of the noninflectional neutral waves are called acoustic modes. Another feature noticeable from comparing Fig. 6 to Fig. 7 is the close proximity of the acoustic submode of an inflectional nth mode (in Fig. 6) to the acoustic noninflectional (n-1)th mode or nth mode of Fig. 7, depending on whether the acoustic submode is to the left or to the right of the vorticity submode. Furthermore, the segments of vorticity submodes tend to form a continuous curve at high M_1, as suggested by Fig. 6.

This and the feature of *near-mode crossing* of the acoustic submodes noted above is best explained by Smith & Brown's (1990) asymptotic result, which illustrates the switching from a vorticity to an acoustic submode along the nth inflectional neutral curve:

$$\left(\alpha - \frac{1}{4}\Gamma_1\right)\left(\alpha - \frac{\pi(4n+1)}{1.788M_1^2}\right) = E(M_1^2, \gamma) \tag{5.1}$$

where Γ_1 stands for $(\ln M_1^2)^{1//2}$, the value of 1.788 was arrived at from $\gamma = 1.40$, and E has a magnitude comparable to $M_1^{-2}\exp(-2\alpha M_1^2)$. Thus the two distinct submodes are separated by an *exponentially small* amount, and the vanishing of the two factors on the left leads respectively to the vorticity and the acoustic submodes. While the vorticity and acoustic submodes differ little in their phase velocities at high M_1, i.e. $c = U_s + O(U_s M_1^{-2})$, they differ substantially in the wave numbers, as the foregoing discussion and (5.1) have indicated. Supported by their analysis, Smith & Brown (1990) propose to classify *instability* modes at *high* M_1, including the neutral waves, into two main kinds: one is the acoustic mode with wave number and growth rate given, respectively, by

$$\alpha = O(nM_1^{-2}), \quad \alpha c_i/U_1 = O(M_1^{-6}\Gamma_1^{-1}), \tag{5.2}$$

and the other is the single "vorticity mode" with

$$\alpha = O(\Gamma_1), \qquad \alpha c_i/U = O(M_1^{-2}\Gamma_1). \tag{5.3}$$

The latter is far more unstable and significant than the acoustic mode at high Mach number (also see Brown et al. 1991). The result (5.2) was also noted by Cowley & Hall (1990). A vorticity mode similar to (5.3) was found in the mixing layer considered by Balsa & Goldstein (1990).

VISCOSITY-TEMPERATURE LAW DEPENDENCE The foregoing asymptotic study was based on a linear viscosity-temperature law. Assuming $\mu \propto \sqrt{T}$, Blackaby et al. (1992) found, instead of (5.2), for the acoustic mode:

$$\alpha = O(nM_1^{-3/2}), \qquad \alpha c_i/U_1 = O(M_1^{-7/2}) \tag{5.4}$$

and for the "vorticity mode", instead of (5.3):

$$\alpha = O(1), \qquad \alpha c_i/U_1 = O(M_1^{-2}). \tag{5.5}$$

The reasons for the change may be traced partly to the difference in the edge-layer behavior of the mean-flow structure for $\mu \propto T$ (Lee & Cheng 1969) and for $\mu \propto T^{\omega}$, $\omega < 1$ (Bush & Cross 1967).

INSTABILITY AT LARGE χ Blackaby et al. also made an instability analysis for the flat-plate problem

in the strong-interaction regime ($\chi \to \infty$), assuming $\mu \propto \sqrt{T}$, and found

$$\alpha = 0(M_1^{7-3\lambda}), \quad \alpha c_i/U_1 = O(M_1^{\lambda-1}) \tag{5.6}$$

where $\lambda = 9\gamma/(6\gamma-1)$, with which both wave number and amplification rates are seen to increase with M_1 for all $\gamma > 1$, quite unlike (5.2)-(5.5) which corresponds to $\chi \to 0$. This is rather surprising since little supporting experimental evidence of instability can be found in the literature in this case.

THE FIRST-MODE/TS WAVES In a triple-deck formalism, Smith (1989) found that the parallel-flow assumption at high M_1 *cannot* hold for TS waves even at a rather low $M_1 = O(Re^{1/16})$, and that, in order to keep the TS waves effectively subsonic for their validity, they must be directed outside the wave-Mach-cone ψ, i.e., $\tan\psi > \sqrt{M_1^2 - 1}$. Cowley & Hall (1990) studied the influence of a shock on the TS waves in the hypersonic boundary layer over a wedge, using a triple-deck approach. To simplify the analysis they introduce a special kind of hypersonic Newtonian approximation, in which the entire shock-layer thickness becomes narrow enough to be comparable to the upper deck. Seddougui et al. (1991) found an adverse wall-cooling influence on the *spatial* growth rate of the (viscous) TS mode, and showed destabilization of the otherwise stable modes.

NONLINEAR EVOLUTION OF THE ACOUSTIC MODE Nonlinear spatial evolution of the unstable waves in the acoustic mode was studied by Goldstein & Wundrow (1990). As seen from Eq. (5.2), the amplification rate of this mode/submode at high M_1 is so weak that even a pressure fluctuation of the order $M_1^{-4}(\ell n M_1)^{-1}$ suffices to initiate the nonlinear evolution.

5.4 Hypersonic Boundary-Layer Transition

Transition prediction requires the identification of the free-stream disturbance field, and determination of the boundary/shear-layer response as well as (linear and nonlinear) amplifications of these internalized disturbances prior to the breakdown to turbulence. Following Malik et al. (1990), the events up to the nonlinear breakdown will be called the stage of "transition onset", to be distinguished from the downstream "transitional zone" that follows.

TRANSITION-ONSET STAGE The e^N method and variants for locating the onset of transition may still work at high M_1 (though with N being substantially reduced from the magic "9"; see Malik et al. 1990); their application requires knowledge of the more dominant first and second (if not all) instability modes, which provide the (spatial) amplification rate σ in

$$N = \ln(A_t/A_o) = \int_{x_o}^{x_t} \sigma(x)dx \tag{5.7}$$

where A_o is the amplitude of the internalized disturbance at the onset of instability and the subscript "t" signifies the end of the transition-onset stage. An alternative to the e^N method is to assign an amplitude *level* to A_t at the end of the onset stage, instead of assigning a level for N which controls the *amplitude ratio* A_t/A_o. This calls for the computation of A_o from the free-stream disturbance amplitude via (linear) receptivity theory. A more viable method appears to be combining the receptivity, linear stability and *secondary* instability theories [in the sense suggested by Herbert (1988)]. Görtler vortices in the boundary layer of a Mach 5 nozzle have been observed by Beckwith & Holly (1981); with Görtler vortices as primary disturbances, for example, the secondary instability waves can develop amplitudes comparable to the primary level at high M_1 (Spall & Malik 1989; Malik & Hussaini 1990) as was found at low M_1.

TRANSITIONAL ZONE MODELLING In modelling the transition-zone flow, the Reynolds averaged Navier-Stokes (RANS) approach deals with an equation system developed from higher-order moments of the *ensemble*-averaged NS equations (e.g. Cebeci & Bradshaw 1988) whereas the Large-eddy

simulation (LES) models the turbulence in the subgrid scale and deals with numerical solutions to the *spatially* averaged NS equations (e.g. Reynolds 1976, Lesieur 1990). Although the LES is still in a developing stage, its prospect as a reliable flow-data source seems high, even for NASP applications (Zang et al. 1989). Using meshes and time steps small enough to resolve the Kolmogoroff scale, direct numerical simulation (DNS) may need no subgrid modelling and yield data with adequate details for some highly idealized, otherwise costly transitional-flow computations. The latter are essential for the LES and RANS calibration. There is also an ONERA/CERT version of the RANS which receives encouraging support from comparison with DNS results (cf. Malik et al. 1990). Among the RANS arsenal in current development is the k-ω model (Wilcox 1988,1991) which captures certain transitional-zone properties well.

Distinct from the RANS and LES approaches, and perhaps more appealing, is the application of a *nonlinear* transition theory by Ng et al. (1990) to the analysis of a *secondary* instability of the (primary) *second* mode on a cylinder at high M_1 in the *early* stages of the transition (cf. Malik et al. 1990, Fig. 17 therein). Their results on the Reyolds-stress profile agrees quite well with the DNS data and reveals the predominance of a secondary instability in the vicinity of the critical layer attributed to a 3-D nonlinear effect. The analysis may explain the "rope-like structure" observed in the vicinity of the critical layer in several transition experiments in hypersonic flows (e.g., Potter & Whitfield 1969).

6. NONEQUILIBRIUM AEROTHERMODYNAMICS: MODELLING AND APPLICATIONS

The works to be examined represent a current research development in high-temperature flow physics and may still be considered far from achieving a methology base with unquestioned certainty; the research has identified nevertheless several vital issues of modelling at the atomic/molecular levels and provided useful engineering estimates.

6.1 Modelling Transition Among Internal States of Atoms & Molecules

THE MASTER EQUATIONS A rational way to derive an equation set for the nonequilibrium thermodynamics of interest is to seek the time rate of population change of atoms/molecules at a specific (energy) state i as the difference between the sum of rates of all collisional (and radiative) transitions that populate the state i and the sum of rates that depopulate the state i. Such a system is commonly referred to as the *Master equations* and will furnish the "source term" in a conservation equation for N_i (the species population at the state i). The transition/emission rate for each collisional/radiative process is to be determined with models/approximations of quantum mechanics of the molecular, atomic and electronic interactions, and with the help of the *detail balance hypothesis* (see e.g., Park 1990, pp. 90-92; Clarke & McChestney 1964, p. 325).

QSS MODEL OF ELECTRONIC STATE Several available computer codes for predicting radiation intensities from flows in thermo-chemical nonequilibrium, such as the NEQRAP and NEQAIR quoted in Park's book, were based on a *quasi-steady-state* (QSS) model of the master equation for the (atomic) electronic states, which determines N_i in terms of a free-electron temperature T_e, and the electron-number density N_e. The latter is determined separately by a rate equation. In NEQAIR, it was assumed that the system could be characterized by three temperatures, T_e, T_v and T; the vibrational temperature T_v is shared by all molecules and the translational temperature T is shared by all heavy particles.

6.2 Vibrational Relaxation/Excitation and Dissociation

The vibration excitation is considered the main channel of energy transmission to the upper level for dissociation and thus controls the dissociation process. For the study of vibrational

nonequilibrium, radiative transitions are considered to be much slower than that by collisions and are deleted from the master equation governing the vibrational transitions (cf., e.g. Park 1990, p. 97).

VIBRATION-TRANSLATION ENERGY EXCHANGE Here, the rates of state-to-state transitions are to be furnished by modelling collision and excitation processes and may lead to quite different results depending on the forms of intermolecular and interatomic potentials and other approximations used. If one considers an end-on colinear (aligned,1-D) collision of a rotationless harmonic-oscillator molecule with an atom or a molecule which has a frozen vibrational energy, assuming also an exponentially decaying interaction potential as in Landau & Teller's (1936) theory, one finds that transitions can occur only to the neighboring states ($v' = v \pm 1$) and a deactivating transition rate proportional to v. This leads to the familiar relaxation equation for the *averaged* vibrational-energy if, in addition, the vibrational levels are assumed to populate according to a Boltzmann distribution at some vibrational temperature T_v, namely,

$$\frac{\partial}{\partial t}\bar{\varepsilon}_v = \tau^{-1}[\bar{\varepsilon}_v^*(T) - \bar{\varepsilon}_v] \tag{6.1}$$

where $\bar{\varepsilon}_v^*$ denotes the average equilibrium vibrational energy at the translational temperature of the (heat-bath) particles, T. The temperature and pressure dependence of the vibrational relaxation times τ for a number of important air-species pairs have been estimated and correlated with experimental data at T up to 5000°K by Millikan & White (1963) and others (see Park 1990).

VIBRATION-VIBRATION ENERGY EXCHANGE Schwartz, Slawsky & Herzfeld (1952) considered the end-on colinear collision model of a diatomic molecule pair, of which the vibrational energies in *both* can be activated, assuming again no rotational energy exchange and a form of (separable) intermolecular potential in this case, as

$$U \propto \exp.[-\alpha(r-\beta_A r_A-\beta_B r_B)] \tag{6.2}$$

where r_A and r_B are the internuclear separations for molecule A and molecule B, respectively, and r is the distance between the mass centers of the two molecules. According to the SSH analysis specialized to a *harmonic oscillator* model, the contribution to the rate of transition through vibrational energy exchange during collisions are found to differ substantially depending on whether the total internal energy change $\Delta E = (E'_A+E'_B) - (E_A + E_B)$ is (nearly) zero or not; the contributions from collisions with $\Delta E = 0$ (resonant case) were seen to be predominant, and thus "preferential". (cf. Park's (1990) discussion, p. 61; the resonant transition may not hold for the high vibrational levels.)

The SSH analysis extended to models with *anharmonic* oscillators and dissociation yields quite different results, made apparent by Sharma's et al. (1988) study elucidated in Park (1990). There, the nonuniform vibrational-energy spacing were calculated for several intermolecular-potential models including the Sorbie-Sorret as well as a 2-term Dunham potentials; the multiple-state transitions $v = v \pm 2$ were also considered. We shall return to this version of SSH extension shortly.

In passing, an earlier study on the anharmonicity by Treanor et al. (1968) should be recalled [also see Rich & Treanor's (1970) review]. Limiting the model to the ladder climbing exchange $v' = v \pm 1$, and assuming that V-T transitions are generally much *slower* than V-V transitions, these authors noted a QSS-type solution to the V-V dominated Master equation

$$N_v \approx N_o e^{-\gamma v} \exp(-E_v/kT) \tag{6.3}$$

where N_o, γ and T may vary slowly with time at rates comparable to the V-T rates. This result can be rewritten as

$$N_v \approx N_o \exp(-vE_1/kT_v)\exp[(vE_1-E_v)/kT] \qquad (6.4)$$

showing at once that for a simple harmonic oscillator the distribution in (6.3) is that of Boltzmann, but for an anharmonic oscillator, the last factor in (6.4) furnishes a needed correction. For $T<T_v$ corresponding to a sudden drop of translational temperature from an equilibrium condition, γ is negative and (6.3) signifies a *population inversion*. The study indicated a relaxation time much shorter than that from the harmonic-oscillator model at the lower-temperature range. Calculations with an extended anharmonic version of the SSH theory allow also molecular rotation of O_2, NO, CO, OH, H_2 and N_2; their application to expanding flows have been carried out recently by Park (1992), Ruffin & Park (1992), and Roany et al. (1992), confirming the essence of the non-Boltzmann distribution (6.4).

ISSUE ON BOTTLENECK IN V-V EXCHANGE Returning now to Sharma's et al. (1988) work for the collisional V-V exchange model of anharmonic oscillators, the overall transition rate coefficients K(v,v+1) and K(v,v+2) as well as K(v,c) were computed up to the vibrational level v = 50 for rotationless N_2 at T = 8000°K, T_v = 4000°K. Here, the K(v,c) is the rate coefficient for the transition from the vibrational state v to the dissociated state unaccounted in Treanor et al. (1968). The case considered with $T>T_v$ corresponds to a sudden heating of the gas, such as that occurring behind a shock. Interestingly, the calculation indicates a vibrational excitation "bottleneck" around v = 20 where K(v,v+1) as well as a second moment of K(v,v') have an extremely low minimum (reproduced in Park 1990, Figs 2.10, 3.3). Using this set of K(v,v') and K(v,c), the time-dependent master equation yields an evolutional solution for N_v which is highly non-Boltzmann with three distinct v-ranges, and evidently this bottleneck inhibits the transfer of vibrational energy to the upper states. With these non-Boltzmann results, Sharma et al. computed the rate of total vibrational population removal, i.e., the forward dissociation rate k_f, as well as the rate of total vibrational-energy loss, or the average *removed* vibrational energy ε_v.

As pointed out by Gonzales & Varghese (1991), these highly interesting results from an extended SSH model are affected, however, by uncertainties related to a number of assumptions made in Sharma's et al. (1988) calculation where corrections for several errors and 3-D effects in the original SSH analysis (Schwartz & Herzfeld 1954, Tanczos 1956) were not made. An issue was also raised on the "distorted wave approximation" implicit in the SSH theory which may not be appropriate for transition involving high relative velocities and multi-quantum transitions (Clarke & McChesney 1964). A more recent study by Landrum & Candler (1991) on vibration-dissociation coupling in N_2 used a corrected and updated version of the SSH theory, including also contributions from colinear collisions of diatoms and atoms, but the important range parameter "α" of the intermolecular potential appears to be improperly determined with the Murrell & Sorbie potential which is appropriate only for the field between bound atoms, according to Gonzales & Varghese. Thus a demonstration of the existence of the bottleneck in question has not been concretely established. It was also pointed out that a recent DSMC calculation by Olynick et al. (1990) using inelastic cross-section data corresponding to the rates used in Sharman et al. (1988) gives no sign of such a bottleneck.

ALTERNATIVE SEMI-CLASSICAL APPROACHES Transition-rate calculations in this case could be improved by using an extension of the semi-classical "N-state method" (Rapp & Kassal 1969) in which the dynamics of the colliding pair is modelled classically while the oscillator motion is modelled quantum-mechanically. The task is rather computationally intensive, only a few among the many needed state-to-state transition rates have been calculated by Gonzales & Varghese (1991, 1992) to-date. Another promising semi-classical approach currently being developed by Kunc (1991) treats the V-T exchange for undissociated diatomic gases based on a multi-center potential model developed earlier (Kunc 1990). The treatment includes a quantum-mechanical interaction of vibration and rotation, retaining however the simplifying features of the 1-D colllisional model. Sample transition

probabilities $P_{j,j-1}$ have been computed for j = 1,4 and 20 for N_2 and O_2. Comparison with the collision numbers for the 1→ 0 transition, Z_{10}, inferred from exisiting experimental data (after adjusting a constant "g" in the theory) show very encouraging agreement in the temperature range T = 1000-6000K°. Comparison of this approach with experiment and with other theories for transition rates at the higher vibrational levels remain to be made.

DIFFUSION THEORY The master equations for the vibrational-state population, allowing also transitions to the unbounded (dissociated) state, may be approximated by an integral equation. With appropriate assumptions, the latter may in turn be reduced to a *diffusion-like* equation (Keck & Carrier 1965) which is amplified here for its theoretical importance in the interpretation of computational and experimental results. If the vibrational energy gap E(v+1)-E(v) is small compared to kT, the master equation for the diatomic molecules may be expressed in an integral equation form [using mostly Park's (1990) notations]

$$N_x^{-1}\frac{\partial}{\partial t}\rho(\mathrm{V}) = \int_0^{\mathrm{v_m}} K(\mathrm{v},\mathrm{v}')[\rho(\mathrm{v}') - \rho(\mathrm{v})]d\mathrm{v}' + K(\mathrm{v},c)[\rho_A\rho_B - \rho(\mathrm{v})] \tag{6.5}$$

where v and v′ are the level number in a suitable unit, N_x is the number density of the colliding partners, ρ is the number density at v-level normalized by its equilibrium value, i.e. $\rho \equiv N_v/N_v^*$, ρ_A and ρ_B are the normalized number density of (free) atoms A and B, and v_m is the maximum v. Two additional requirements are needed in the diffusion theory; they amount to (i) the rate K(v,v′) is large only in the vicinity of v′ = v, (ii) K(v,c) is appreciable only at those upper states near the dissociation limit. Note that the typical mid-level vibrational energy is of the order D, and that in most cases of interest kT<<D. This, together with the assumption required for the integral form of the Master equation, means

$$\Delta E \equiv E(v+1)\text{-}E(v) << kT << D \tag{6.6}$$

The kernel K(v,v′) is sharply peaked under assumption (i), this allows simplifications of (6.5) to

$$N_x^{-1}\frac{\partial}{\partial t}\rho(\mathrm{v}) = \frac{\partial}{\partial \mathrm{v}}\left[M\frac{\partial}{\partial \mathrm{v}}\rho(\mathrm{v})\right] + K(\mathrm{v},c)[\rho_A\rho_B - \rho(\mathrm{v})] \tag{6.7}$$

where M is a transition moment

$$M(\mathrm{v}) \equiv \int_{-\infty}^{\infty} K(\mathrm{v},\mathrm{v}+\xi)\xi^2 d\xi \tag{6.8}$$

If one excludes those high lying v-states with energy E(v) close to the dissociation limit D, then, by virtue of the assumption (ii) appropriate under (6.6), a diffusion equation follows

$$N_x^{-1}\frac{\partial}{\partial t}\rho(\mathrm{v}) = \frac{\partial}{\partial \mathrm{v}}\left[M\frac{\partial}{\partial \mathrm{v}}\rho(\mathrm{v})\right] \tag{6.9}$$

The boundary condition at v = 0 is obviously $\partial\rho/\partial v = 0$ since no molecules can cross this boundary. The upper boundary condition at $v \to v_m$ was furnished by Keck & Carrier as

$$M\frac{\partial\rho}{\partial \mathrm{v}} = (\rho_A\rho_B - \rho)\int_0^{\mathrm{v_m}} K(\mathrm{v},c)d\mathrm{v} \tag{6.10}$$

An ambiguity then appears since the right member of (6.10) is also seen to be the net formation rate of molecules from atoms. A more in-depth discussion on the boundary conditions is given in Park's recent (1992) paper. Equation (6.9) would show that a vanishingly small diffusion coefficient M occurring at some mid level would inhibit the upward population migration to the dissociation level and would signify a "bottleneck" noted earlier, and the M(v) in the example of sudden heating of N_2 in Sharma's et al. (1988) study did reveal an extremely low minimum. The latter result would have made great theoretical impact if not for the several uncertainties brought out earlier.

A rather encouraging application of the diffusion theory has been made recently by Lee (1992) who considers a model of energy exchange of vibrational oscillators with an *electron* heat bath in the absence of dissociation. This model has been considered important in the study of highly ionized reentry flow (Lee 1985). Reasonable agreement of the diffusion model with the original discrete master equation in the sudden-heating case is demonstrated here; non-Boltzmann distributions were shown at an earlier stage of the transient, but a "bottleneck" in $K(v_1 v')$ was not evident.

6.3 *Applications, Validation and Assessment*

MULTIPLE-TEMPERATURE MODELS AND REACTION RATES The extensive study of the vibrational transition models has led invariably to an appreciation of the multiple-temperature concept in nonequilibrium aerothermodynamics. These improvements in concept take the forms of allowing several independent temperatures, namely, the translational-rotational temperature T *shared* among heavy particles, the vibrational temperature T_v *shared* by all molecules and (depending on the requirement) the electron-electronic temperature T_e; these temperatures enter in the empirical rate formulas to reflect on the impact of T, T_v and/or T_e suggested by the model studies. Note must be taken to the rate of vibrational energy change (per unit volume) due to collision which may be evaluated as a sum contributed by three sources: (i) the Landau-Teller form for V-T and V-V transitions modified by a factor depending on T_v and T, (ii) vibrational excitation contributed by electronic impact (significant for N_2), (iii) vibrational energy removal/addition due to dissociated/recombination, with the energy per molecule $\bar{\varepsilon}_v$ based on some preferential dissociation model. This sum then enters as a source term in the conservation PDE governing E_v. Similarly, the rate of the electronic energy change E_e owing to the kinetic process is contributed by seven terms resulting from electronic excitation, ionization, ionic recombination, radiation, etc. This rate enters again as a source term in the conservation PDE for E_e.

More empiricism is found in the attempt to modify the pre-exponential temperature dependence in the forward reaction rate k_f, namely, replacing T by the product of an *average* suggested by Park

$$T_a = T_v^q T^{1-q} \tag{6.11}$$

where q varies between 0 and 0.5 in practice. The lack of adequate experimental data to determine the constants and exponents of the rates represent an uncertainty in the study which may therefore be considered *qualitative at best*. Another area of ambiguity concerns transport properties of the gas mixture and its simplification (Yos 1963, Wilke 1950), which has never been critically tested or ascertained at the elevated temperature range of interest. The need for their scrutiny is made apparent by the example of iodine considered by Kang & Kunc (1990) noted earlier.

CONVECTIVE AND RADIATIVE HEATINGS Gupta (1987) studied the thermochemical and radiative properties of the shock layer during the Fire II reentry study carried out by a Space Shuttle experiment (Cauchon 1966); solutions were obtained for NS equations with nonequilibrium chemistry, and for viscous shock-layer (VSL) equations but with equilibrium chemistry. Except at altitudes higher than 80 km, the Fire II data of radiative intensities, heat fluxes agree reasonably well with the equilibrium VSL solutions for a fully catalytic surface as well as the inviscid shock-layer and boundary-layer analyses of Sutton (1984). In a code-calibration study, Gnoffo (1990) applied the LAURA code using park's 11-species model with $T_a = \sqrt{T_v T}$ to predict convective heat transfer rate of the Fire II test during the early period (corresponding to 11.3 km/sec speed and altitude 85-67 km). Good agreement with flight test data are found although the heating rates in this range are too small compared to those at the lower altitudes to be of significance.

In a proposed Aeroassisted Flight Experiment (AFE), Hamilton et al. (1991) predicted the

stagnation-point heating history of a fully catalytic heat shield with 2.2 meter nose radius using an 11-species nonequilibrium air chemistry and the VSL approximation. Peak convective heating in this case occurs at 78 km altitude at speed 9.2 km/sec and the predicted value reaches 0.5 mega watt/(meter)^2 (which is believed to be the limit for the reusable tile on the Space Shuttle). However, this VSL analysis ignores the "shock-slip correction" which would result in a 50% reduction of the peak value (cf. §8).

ENTRY INTO MARTIAN ATMOSPHERE AND RETURN Radiative heating will dominate the surface heat flux at considerably higher reentry velocities and at lower altitudes and on a larger body, such as during an aerobraking return from Mars. A coupled radiation and ablation injection model of the nonequilibrium viscous shock layer was used in a reentry heating study by Gupta et al. (1990) in the latter case, assuming a speed 16-8 km/sec, altitude 80-65 km, and a nose radius 3m. The study extended an earlier work of Moss (1976) and assessed the impact of using different transport and thermodynamic properties, and also different radiation models and, interestingly, showed the adequacy of a universal Lewis number 1.40. Over the speed range 12-16 km/sec, the wall heating rate was found to vary from 2.5 to 11 MW/m^2, of which radiation contributes 40-70%; the effectiveness of the albative injection of carbon-phenolic is unclear from the study. Entry into the Martian atmosphere represents a different aerothermal environment where CO_2(97%) and N_2(3%) are the main constituents; estimates for entry vehicles with nose radii varying from 1 to 23 meters indicate the need of considering a speed range 6-12 km/sec at altitude 30-50 km. Candler (1990) and Park et al. (1991) have studied the nonequilibrium nature of this problem. Candler's NS calculations based on an 8-species chemistry without ionization reveals *near thermo-chemical equilibrium* in most parts of the shock layer, attributed to the rather fast CO_2 vibrational relaxation. Applying a computationally more efficient VSL analysis to this problem, Gupta et al. (1991) assumed a full thermochemical equilibrium but allowed coupling of the shock-layer thermodynamics to the radiative cooling. Their results at the lower speed range (6-6.5 km/sec) support Candler's (1990) observation on chemical equilibrium. Convective heat transfers at 8 km/sec speed contributes to 60% of the total heat flux for the 1 m.nose radius, and to 23% for the 23 m.nose radius; at 12 km/sec speed, it amounts to only 40% for the 1m. nose and 2.4% for the 23 m nose.

ELECTRON-NUMBER DENSITY A series of instrumented probes, called the RAM-C tests, were flown at speed 7.65 km/sec and altitudes 71-81 km to measure electron-number density around a spere-cone with a 0.152 m nose radius (Jones & Cross 1972). Gnoffo (1990) compared his LAURA calculations of electron-number density profile using two sets of chemical kinetic rates with the data measured by a Langmuir-probe rake. Only qualitative agreement can be achieved (cf. Gnoffo 1990, Fig. 13). Whereas, an earlier VSL calculation by Kang et al. (1973) showed a better agreement with the measured data. The discrepancy was believed to have resulted from a fully catalytic surface assumed in the LAURA calculation inappropriate for a Teflon coated afterbody.

Candler & MacCormack (1988) assumed a non-catalytic wall in an earlier NS calculation for this case and indeed found reasonable agreement in the electron-number density with the RAM-C microwave-reflectometer data measured along the cone afterbody (cf. Figs. 2-4 therein). The basic numerical procedure of the last work has been noted earlier in §3; two sets of chemical kinetic models were tested, one consists of five species N_2, O_2, NO, N and O, the other consists of two more species NO^+ and e^-. The electron density in the 5-species set was generated by a special quasi-steady approximation which proved to be inadequate. Treatments of nonequilibrium flow models are similar to those of Lee (1985) and Park (1990). The program allowed distinct vibrational temperatures for different molecular species, which turned out to be very close to one another, thus supporting Park's idea of a common T_v shared by all molecules.

Using a two-temperature version of the LAURA code, Greendyke et al. (1992) carried out a

parametric study of the unknown constants/exponents in the nonequilibrium thermochemical models and their impact on electron-number density prediction for the AFE experiment. Variations are considered in the reference ionization potential of N and selection of rate constants from among Kang & Dunn (1972), Park (1987,1990), and their updates, including the option of using Gupta's et al. (1990) equilibrium constant, and also options of imposing limiting cross sections for vibrational excitation. A value of the exponent q in (6.11) proposed by Hansen (1991), $q = 0.1+0.4(T_v/T)$, were also considered; it appears to yield only minor changes in this case. The calculations made for an AFE model (2.16m nose radius at 78-81 km altitude, velocity 9.7-8.9 km/sec) reveals significant variations in the rates of electron-impact ionization with correspondingly large differences in the location and magnitude of the peak electron density. The severity of an electron avalanche associated with changes in these models was noted.

MORE PARAMETRIC STUDIES Another and perhaps a more extensive parametric study was made earlier by Hartung et al. (1991), Mitcheltree (1991) and Hartung (1991) using the two-temperature version of the LAURA code. Hartung et al. studied radiative emission profiles and radiation spectra in the stagnation region for conditions corresponding to a FIRE II flight experiment (altitude 76-85 km, speed 11.4 km/sec, nose radius 0.75m). The radiation model used was the Langley Optimized Radiative Nonequilibrium (LORAN) code which proves to differ little from Park's NEQAIR in results. The sensitivity study includes again the choice of the exponent q in (6.11) for the dissociation rate, and of the limiting vibrational relaxation cross section, both of which were shown to be critical. Mitcheltree (1991) examines LAURA solutions of translational and vibrational temperatures, electron-number density, O_2-concentration as well as convective and radiative surface heating rates. The flow condition in the study corresponds to an aerobrake of 1-m nose radius at speed 12 km/sec, 80 km altitude. Rate parameters variations are seen to have an effect, as large as a factor of three, on the ionization degree and radiative heating. The results based on Park's (1987, 1989, 1990) rate sets were seen to be affected little by using Gupta's et al. (1990) equilibrium constant; Hansen's model (6.12) appears to give results virtually identical to that for q = 0 in (6.11).

Hartung (1991) pointed out that the procedure in Park's NEQAIR code may lead to a negative excitation temperature for a bound-free transition which is avoided in LORAN. Comparison of predicted emission spectrum in the visible range from LORAN with an AVCO shock tube experiment (Allen 1962) at the condition corresponding to the peak radiation point does not however appear to be as good as expected, thus requiring further study. On the other hand, there has been better agreement of the NEQAIR prediction with the AVCO emission measurement found earlier by Park both in equilibrium and nonequilibrium regions (1989; cf. also Park 1990, Figs. 8.24). The comparison is reproduced in Figs. 9a,b where the dash curves are results from DSMC models to be discussed in §8.

7. FLUID DYNAMIC PROBLEMS OF HYPERSONIC AIR BREATHING PROPULSION

7.1 Preliminary Remarks

Reviews on major developments in the theory and design of hypersonic air-breathing propulsions and their key fluid dynamic problems have been cited earlier in §§1-3. The following will discuss some recent works on the combustion fluid dynamics. Unlike the flow chemistry of external aerodynamics, the overall combustion chemistry of interest is heat releasing (exothermic) and its interaction with the fluid dynamics giving rise to many important features of supersonic combustion. Also unlike the flow chemistry at low speed, the resident (flow-transit) time in a supersonic combustion may *not* be long compared to the characteristic time of the chemical reaction so that the energy conversion of interest

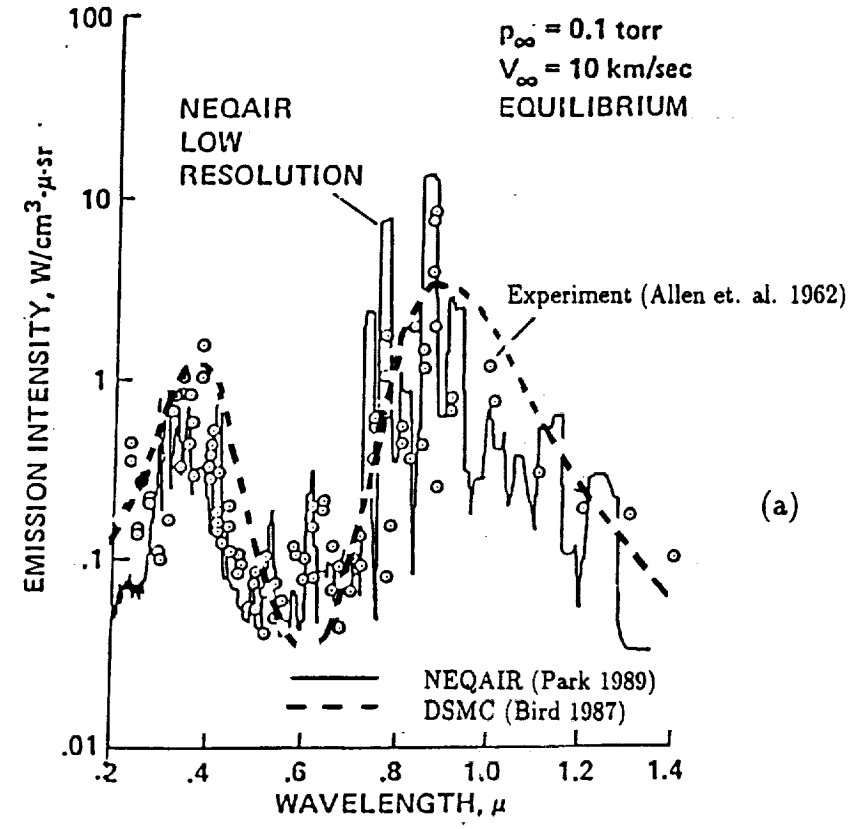

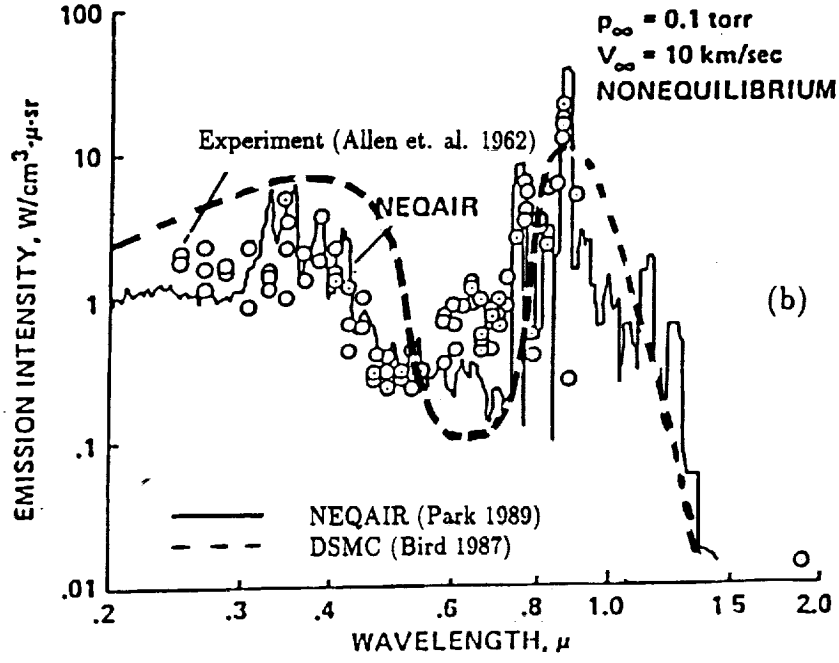

Fig. 9 Comparison of calculated and measured spectra for air behind a shock advancing at 10Km/sec. in a shock-tube section with initially pressure 0.10 torr (from Park 1989) : (a) near equilibrium region, (b) nonequilibrium. Emission spetra prediction based on Bird's (1987) DSMC-VHS model are shown as dashes.

is determined by the *finite-rate* chemistry and may depend also critically on the fluid-mechanic mixing process (Ferri 1973, Billig 1992).

The propulsive performance estimates from the late 1950's are nearly identical to those that are being calculated more than thirty years later, according to Billig (1992); several long recognized problems in supersonic combustion research still remain open today. Some of the observations and design guidelines offered in Billig's (1992) review may also prove helpful to newcomers in the field. The fuel specific impulse Isp (sec) is related to the propulsive efficiency η_p, the vehicle speed V and the caloric fuel value H as $Isp = H\eta_p/V$. Studies up to the mid 1970's indicated that at Mach 6, Isp value of H_2 fuel is about 3000 sec, being almost twice the Borane value (1600 sec) for either ramjet or scramjet, and, at Mach 10, the scramjet is clearly superior with an estimated Isp slightly more than 2000 sec for H_2 and 1000 sec for borane (Waltrup et al. 1976, fig. 1). This substantiates a propulsive efficiency of η_p of 0.5-0.6 in the Mach-number range 6-10 anticipated in early studies (cf. §2.1).

In passing, we recall the severe shock interference heating found at the cowl lip of a scramjet engine noted in §3 where the high heating rate 30 times the normal stagnation point value has not yet been closely predicted to the best of the writer's knowledge.

7.2 Scramjet Mixing-Combustion Studies

H_2-AIR MIXING AND COMBUSTION Eckland & Northam (1992) studied the effects of certain geometric parameters on a combustor performance under conditions corresponding to M_∞ = 5-7. The basic problems analyzed was the mixing and combustion of an H_2 round jet injected (normally) from a hole downstream of a step and the effectiveness of the equivalence ratio ER, wall deflection angle θ, and the stagnation temperature T_o in controlling the chemical and mixing efficiencies. (The ER is defined as the ratio of injected fuel to that is required for the stoichiometric reaction.) NASA Langley's Reynolds-averaged NS code SPARK was used with finite-rate chemistry of six reacting and one inert species. Several measured mixing and chemical efficiencies, defined in the paper, were determined and indicate the important roles of chemical kinetics at higher M_∞. The nozzle hole shape is known to significantly alter the jet mixing rate at low speed (Ho & Gutmark 1987), its potential in enhancing mixing in supersonic flows remains to be ascertained.

Another parametric 3-D computational study was made by Kamath et al. (1991) seeking the influence of the ER value and flight Mach number M_∞ on the performance for a conceptual scramjet combustor at M_∞ = 3-20, which consists of a ramp and slot fuel injectors. A parabolized version of a SHIP3D (NS) code with a k-ω turbulence closure model (Coakley 1983) was used; chemical equilibrium was however assumed. Significant increase in the mixing efficiency with ramp injection angle, ramp angle and ramp sweep angle were found.

It is unclear how sensitive is the solution to the turbulence diffusion model used and how an alternative 3-D turbulence model may affect the result. Some of these issues on turbulence mixing and thrust augmentation techniques applicable to scramjets were discussed in Kumar et al. (1989).

SLOT AND CONTOUR-WALL INJECTOR MIXINGS A number of recent studies focus on fluid dynamic means of increasing mixing efficiency in scramjet combustion (and to compensate for the less efficient mixing in the case of an axial injector). Of considerable fluid mechanic interest are a series of experimental and computational investigations of shock enhanced mixing, exploiting the principle of *baroclinic* ($\Delta\rho x\Delta p$) vorticity production (Marble et al. 1987,1990) and its application to contoured wall fuel injectors (Waitzel et al. 1991,1992). The small sketches in Fig. 10 describe the basic model geometry. To simulate mixing of air with a light gas, helium was injected axially at a speed comparable to that of the air flow. The experiments were conducted in a NASA Langley Mach 6 wind tunnel. The numerical simulations were performed with the SPARK 3D code, assuming laminar

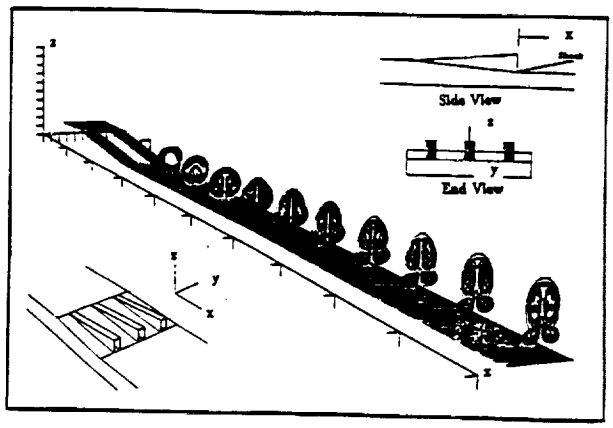

Fig. 10 Computed contours of constant helium mass fraction downstream of a contoured wall fuel injector in a Mach 6 wind tunnel at $Re \sim 2\times10^7$ (Waitzel et al 1992). The shear layer at the injector exit was assumed in this example to have a boundary-layer to injector-height ratio of 0.20.

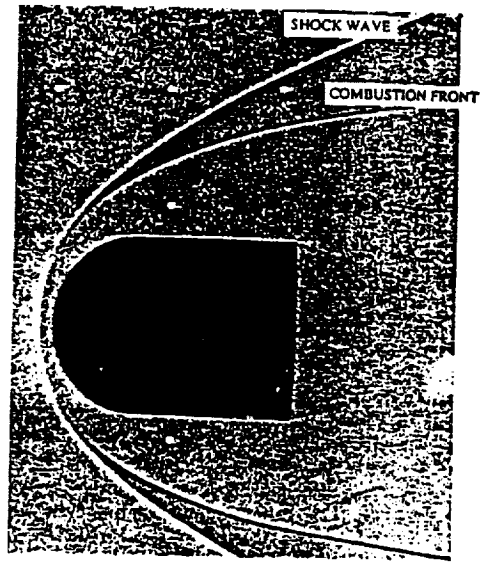

Fig. 11 Schlieren photograph of shock deflagration around a blunt obstacle at superdetonation speed in a stoichiometric H_2-air mixture (reproduced from Lee & Deiwert 1990, photo-record originally from Lehr 1972).

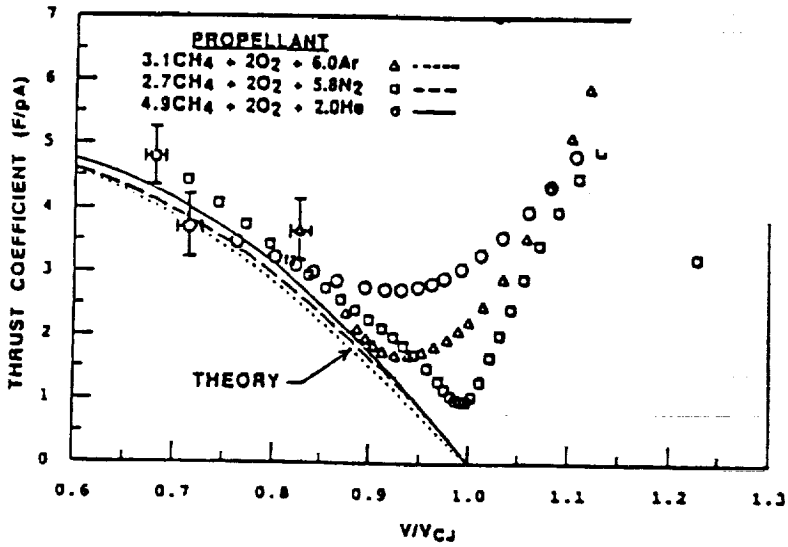

Fig. 12 Variation of thrust coefficient of a ram accelerator with velocity ratio V/V_{CJ} in three different propellant mixture (from Hertzberg et al 1991)

flows. Thus the analysis was expected to capture only large-scale kinematical processes. The key player in the baroclinic vorticity production is the oblique recompression shock right behind the injector; its intersection with the (non-parallel) high density gradient at the fuel-air interface determine the baroclinic growth of the axial vorticity which is expected to enhance mixing. The cross-flow patterns from computation (helium mass-fraction contours) and those from wind-tunnel measurement (pitot pressure contours at a slightly higher injection velocity) were broadly in accord. An example of the computed cross-flow patterns at successive downstream stations are reproduced in Fig. 10. The effects of incoming boundary layer height, injector spacing and other parameters were investigated.

The injector performance in the last cited study was observed to be strongly dependent on the thickened hypersonic boundary layer on the ramp. Such a pronounced viscous influence was quite clearly shown in an earlier computational study of the hypersonic flow through a narrow expansion slot by Hung & Barth (1990) who applied a finite volume, TVD version of the thin-layer ARC 3D code (cf. §3) to the flow about an injector which was comparable to those sketched in the last figure, but only the viscous flow blockage effect in the narrow expansion slot (between neighboring injectors) upstream of the mixing zone was investigated. Results obtained for Mach number 5 and Re of 10^5 indicates a significant (60%) total pressure loss with a surprisingly minor loss in mass flux (12%). Wall cooling is shown to reduce the loss and increase the flow expansion substantially.

7.3 Premixed Shock-Induced Combustion

Steady and unsteady detonation waves involving a premixed fuel-air combustion behind a shock is a classical topic in combustion theory (Karman et al. 1958, Williams 1985). The following will discuss problems in recent studies with detonation waves in hypersonic flows.

PREMIXED COMBUSTION ABOUT A SHOCK HOLDER In the validation study for their F3D/Chem computer code, Lee 7 Deiwert (1990) analyzed the supersonic combustion of a stoichiometric H_2-air mixture around a blunt obstacle and compared the density field with the photorecord from Lehr's (1972) early experiment. The finite-rate flow chemistry with seven active and one inert species was incorporated into an implicit flux-vector splitting code (Ying's F3D). Applying to an example with a 0.75cm nose radius at pressure 0.42 atm and speed 2.6 km/sec (M_1 = 6.46), the present method reproduced results from a number of existing codes, but cannot reproduce experimental data with any of the three selected sets of rate coefficients. Lehr's Schlieren photograph shown in Fig. 11 reveals two distinct density demarcations. The inner demarcation was interpreted to be a flame combustion front. This front approaches closely the bow shock in the blunter part of the shock delimited by the sonic points (right behind the shock), where the reaction is fast enough to provide a relatively thin detonation-wave structure. At the sonic point, the Chapman-Jouguet condition will not allow local heat release, and beyond the sonic point on the outer part of the shock, heat addition along the streamline is again possible but at a much lower rate, owing to the critical temperature dependence of the reaction rates. This results in a much longer "ignition delay" which may explain the marked departure of this part of the combustion front, which could also be called "deflagration wave". The failure to capture this front in computation could be caused by the omission of HO_2 and H_2O_2, and to ignoring the influence of the nonequilibrium molecular vibration on the reaction rates, familiar from the preceding discussion in §6. The authors note specifically that an exceptionally long induction time preceding H_2 dissociation may have occurred in the flow. More recently, this computational problem is re-examined in Wilson & MacCormack (1992), implementing the MacCormack-Candler (1989) procedure discussed earlier with an adaptive grid, which appears to be successful in capturing the deflagration front. Only the inviscid model has been considered.

RAM ACCELERATOR AND DETONATION WAVES The "ram accelerator" is a projectile launcher virtually equivalent to a scramjet-in-tube, with propulsive cycles similar to that generating thrust in an

airbreathing ram/scramjet (Hertzberg et al. 1988,1991). Fuel premixed with oxygen and inert gas components in the tube is heated and ignited by a shock-wave system attached to the high-speed projectile which derives thrust from the combustion. The performance of such a device, and the thermodynamic states of the combustible propellant gas can be studied by a 1-D analysis as for a stationary Chapman-Jouguet detonation wave, but with the inclusion of a thrust term. As a result, the (relative) incoming velocity V that allows the maximum heat addition can no longer be the Chapman-Jouguet (C-J) velocity, but becomes generally lower for a nonvanishing thrust. Figure 12, reproduced from Hertzberg et al. (1991) as a representative sample, compares the 1-D theory (dotted, dashed and solid curves) with data inferred from ram-accelerator measurements for three sets of premixed propellants (symbols), assuming that the exothermic reactions can carry to their completion. The comparison supports the expectation of the 1-D thrust generation analysis, but at speed approaching and beyond the C-J value, experimental data show significant thrust generation which cannot be explained by the simple theory. Computational efforts were being made to attack the problem (Chuck et al. 1991). The thrust generation in the trans-detonation regime and beyond are yet to be investigated theoretically.

COMPUTATIONAL SINGULAR PERTURBATION There have been a few CFD methods which address the complex "stiff" equations of nonequilibrium combustion and reacting flows using fractional time steps and implicit/coupled strategies with a varying degree of success. A recent approach called Computational Singular Perturbation (CSP) recognizes the needs to address the nature of the "many-time-scale problems" and to design algorithm for deriving computationally time-resolved, simplified kinetic models from the otherwise complex reaction system (Lam et acl. 1989, Lam & Goussis 1990). The work perceives the concentrations of N species as components of a vector y and their governing kinetic equation as

$$\frac{d}{dt}y = G(y) \tag{7.1}$$

with the global reaction rate G being contributed by the M elementary reactions

$$G = \sum_{j=1}^{M} F^j S_j \tag{7.2}$$

where F^j is the reaction rate of the jth elementary reaction and S_j is the stoichiometric (column) vector. The key idea of the CSP is to project the M terms in (7.2) into N *modes* associated with a desirable system of N linearly independent *basis* vectors α_i's. Each of α_i contains a suitably chosen time scale, so that fast and slow modes can be grouped and distinguished. In principle, we can express the right-hand member in α_i's so that

$$\frac{d}{dt}y = \sum_{i=1}^{N} f^i \alpha_i \tag{7.3}$$

Its success would lie in finding a way to *decouple* the modes through f^i so that the amplitude of the uncoupled mode may evolve with its own characteristic time. The numerical procedure must deal with the convergence problem in its search for the normal mode of interest, apart from finding a robust method to identify the basis vector set which will not stay fixed and is highly temperature sensitive. The approach has been applied to methane combustion and also to dissociating hypersonic flows; it also has proven helpful in identifying the more important reactions in a complex, large system (Goussis et al. 1990, Gnoffo 1990).

8. RAREFIED HYPERSONIC FLOW AND CONTINUUM EXTENSION

Owing to space limitation, the following will limit the discussion on rarefied flow to a minimum, and give preference to the issues on the continumm extension pertaining to fluid dynamic interest. Broader perspectives on RGD have been offered in earlier volumes of the Annual Review (Sherman 1969, Kogan 1973, Bird 1978, Muntz 1989) and more recent works and reviews can be found in the 1989 RDG Proceedings (Beylich 1990) and the forthcoming 1992 RGD Proceedings.

8.1 DSMC as a Predictive Tool

PRELIMINARY REMARKS The basic ideas of the DSMC method and numerical procedures were described in Bird's (1976) monograph, and the underlying idea elucidated in several extensive reviews (Bird 1978, 1979, 1985, 1989). While the statistical errors present in a solution are expected to be proportional to the square root of the total number of simulated particles, i.e., $\sqrt{N}$, an essential feature of the DSMC procedure is that the computation work is proportional to only the first power of N. The computer resource for a 2-D analysis is generally manageable in many institutes and universities, but is still much larger than that required for a NS calculation. Variants of this method have been developed for improved computational performance with vector-and parallel-processing computer architectures (Furlani & Lordi 1989, Baganoff & McDonald 1990, Boyd 1991, Wilmoth 1991, McDonald 1991).

VARIABLE-HARD-SPHERE MODEL AND INELASTIC COLLISIONS A novel feature which greatly increases the computing speed of Bird's DSMC program is the variable-hard-sphere (VHS) model which treats the interaction of the molecules as a collision between two rigid spheres. This allows the post-collision relative velocity to be sampled from a uniform distribution in solid angle while the sphere radius is allowed to vary with the relative velocity c_r so as to preserve the correct viscosity-temperature relation in translational equilibrium, i.e., $\sigma \propto c_r^{-2\omega}$.

Extensions to molecules with rotational and vibration excitations have been made with the Borgnakke-Larsen (BL) (1975) phenomenological model, in which a fraction of the collisions is assumed elastic and the remainder inelastic. New values of the internal and translational energies are then sampled from an *equilibrium* distribution to be taken as the post-collision particle properties pertaining to the inelastic fraction. The characteristic collision number, Z, for the internal energy relaxation is roughly taken to be the reciprocal of the inelastic-collision fraction and may be chosen to match the relaxation-time estimated from experiment. The collision number Z has been commonly taken to be 5 for rotation and 50 for vibration. In their DSMC calculation for a shock front, Olynick et al. (1991) took into account the temperature and pressure dependence on the relaxation collision number in accordance with the rates used in the continuum model. Additionally, Boyd (1990) derived a velocity-dependent collision number which gives results in accordance with those of Parker (1959).

Bypassing the BL phenomenological model, Boyd (1991) proposed a vibrational relaxation model for VHS application by modifying the Landau-Teller theory. It succeeds in determining vibrational cross sections for (one-step) activation and deactivation, which turn out to be *independent* of the intermolecular collision model. The model compared well with one experiment and represents a more detailed predicting method than the BL phenomenological model. An alternative modification of the BL model was offered by Chung et al. (1991) for a mixture which assumes a combining rule for the effective collision cross section.

CHEMICAL REACTION AND RADIATION A form of collision theory of chemical physics that is consistent with the VHS model was used to convert the temperature-dependent rate constants to collision-energy dependent *reaction cross sections* Ambiguity in modelling the three-body collision arises. The latter, however, may not be of great concern for DSMC applications since the *binary-scaling* law prevails in most cases of nonequilibrium flow of interest (Gibson & Marrone 1962, Hall et al. 1962, Anderson

1989). A BL-type equilibrium distribution for the reaction products was again assumed; whether the model may allow vibrational-temperature dependence of the reaction rate is unclear.

A similar idea was adopted in an extension of the DSMC to nonequilibrium flows with radiation (Bird 1987, Moss et al. 1988). Apart from issues on the BL phenomenological model, the task of tracking the large number of electronic states and of adjusting the constants for each rate to match data from available experiments and other continuum-based sets would appear insurmountable. Nevertheless, this task was accomplished and documented in detail. As a validation, Bird compared the spectral distribution of emitted radiation determined from an 11-species air-chemistry calculation for an example corresponding to an AVCO experiment shown earlier in Figs. 9a,b, in which the thick dashes represent Bird's (1987) results and appear to capture the trends well even in the nonequilibrium flow region. Inasmuch as the number of adjustable constants in the program is huge, an extensive sensitivity study is in order. Such an investigation was performed in part in Carlson & Hassan's (1991) study where a scheme was introduced to determine the relaxation collision number "Z_e" for the electronic-state excitation, which may reduce the degree of empiricism in the existing DSMC radiation model.

Bird's DSMC radiation model was applied by Moss et al. (1988) to predict the history of radiative and convective heating on an AFE vehicle which was investigated earlier by Hamilton et al. (1991) using various versions of continuum models (cf. §6) and corresponds to altitude 78-90 km and velocity 7.6-9.9 km/sec. The study indicates that the radiative heating is negligible compared to the convective heating; it becomes noticeable but still small during the peak heating period, where the stagnation convective and radiative heat fluxes are 0.19-0.21 MW/m^2 and .03-.04 MW/m^2, respectively, which are lower than the corresponding continuum VSL predictions by a factor of 0.40.

8.2 More DSMC Calculations and Comparisons With Experiments

A number of comparisons of recent DSMC calculations with experiments were reported in the Proceedings of the 17th International Symposium of Rarefied Gas Dynamics (Beylich 1990). There are several notable examples of comparisons from more recent studies.

RAREFIED FLOW IN NOZZLES The steady expansion of nitrogen from a 20° mozzle to a near-vacuum (with throat Knudsen number 2.3×10^{-3}) was investigated experimentally and computationally using NS and DSMC (Boyd et al. 1991). Consistently good comparisons were found between DSMC calculations and Pitot pressure and flow angle measurements in and out of the nozzle. Whereas the solution is sensitive to the surface-interaction model, the fully diffuse wall model appears to be quite satisfactory.

SHOCK INTERFERENCE ANALYZED BY DSMC The severe interference heating problem at a scramjet cowl lip noted in §3 (Fig. 2), the Edney Type IV problem, was attacked by Carlson & Wilmoth (1992) with DSMC calculations using 400,000 simulated molecules. The peak heating rate obtained appeared to be considerably lower than the experimental value $q/q_o \sim 30$ (Wieting 1990). As the author noted, the grid/cell system employed may not be adequate, and a full NS calculation should have been made in this case.

SPHERE DRAG AND WAKE STRUCTURE DSMC calculations were made by Dogra et al. (1992) to compare with hypersonic sphere drags at low Knudsen numbers (M_∞ = 11-13, Kn = 0.01-0.09) measured by Legg & Koppenwaller (1970). The adequacy of the cell size and DSMC's capability for describing unsteady separation are open to question.

PLUME INTERACTION, DELTA WING, AFE VEHICLE DSMC calculations and experiments on plume-freestream interaction were made by Campbell (1991); comparison in density distribution showed

qualitative agreement. A 3-D version of DSMC calculations for a delta wing (Celenligil & Moss 1991) were compared to a DLR wind-tunnel experiment at Mach 8.9, Knudsen number 0.02-2.0. Good agreement was found in lift, drag and surface heating rate; the surface temperature is believed to be near the stagnation value in this case. The aerodynamics of a "viscous optimized waverider" (cf. §2) in the rarefied gas dynamic regime was examined with DSMC calculations by Rault (1992). Using the F3 program of Bird (1990a,b), Rault gave a L/D of 0.24 at Mach 25, 100 km altitude (Kn = 0.01). It appears to be inferior to the delta wing last mentioned which has a L/D better than 0.5 at Kn less than 0.10. Interestingly, a 3-D DSMC calculation made recently for the very blunt AFE configuration (Celenligil et al. 1991) gave L/D = 0.212 at 100 km, not far from Rault's value 0.24.

8.3 More Detailed Validation of DSMC

A more critical assessment of the DSMC method is to sample for the velocity-distribution functions f(u,v,w) and compare them with corresponding experimental data. Several sets of unpublished data for argon and helium ideal for this purpose were obtained earlier by E.P. Muntz for the *partially integrated f* within the shock-transition zone (inferred from measured intensity profiles of predominantly Doppler-broadened emission lines excited by an electron beam, known as electron fluorescence technique). Difficulties were encountered, however, in identifying the precise location at which each measurement was made, owing to a number of uncertainties related to the instrument and to the flow field nonuniformity. Thus the comparison study (Erwin et al. 1991; Pham-Van-Diep et al. 1989, 1991) served as a validation of the experiment procedure as well, especially since a *convolving* calculation procedure was adopted in some cases to identify the location that best fits a particular experimentally determined (parallel or perpendicular) distribution function. In their analysis, Erwin et al. used differential cross sections based on Maitland-Smith (1981) potential, replacing the VHS collision model, which fits experimental viscosity data slightly better than other forms do.

Two sets of predicted and experimental velocity distribution functions for a Mach 25 shock in helium are reproduced from Pham-Van-Diep et al. (1989) and shown in Figs. 13a,b, where the convolved parallel and perpendicular distributions

$$f_{\parallel}(u) = \int\int f\,dv\,dw, \qquad f_{\perp}(v) = \int\int f\,du\,dw \tag{8.1}$$

are drawn in solid curves and dashes, respectively, with the corresponding experimental data shown as open circles and open triangles. The data set of Fig. 13a were identified with a location where the number density ratio $\tilde{n} \equiv (n-n_1)/n_2-n_1)$ is 0.285, and the set of Fig. 13b pertaining to a further downstream station where $\tilde{n} = 0.565$. Similarly detailed agreement was found with helium at Mach 1.59 and argon at Mach 7.18 (Erwin et al. 1991). These close comparisons indicate the remarkable ability of DSMC to predict population of scattered atoms in this highly nonequilibrium state; they also reveal unmistakably the Mott-Smith (1951) type bimodal-like distribution, which signifies the persistent influence of the upstream and downstream states. It remains to be seen if the VHS version of the DSMC may also produce similarly encouraging comparison. [A preliminary study with VHS (Muntz et al. 1991) indicated general agreement with noticeable differences in the vicinity of the $f_{\perp}$ maximum.]

8.4 Continuum Extension to Rarefied Hypersonic Flow

The foregoing examples have demonstrated that the DSMC method can treat problems normally handled by the NS-based equations, but it demands large and costly computer resources. For example, one of Carlson et al. (1992) DSMC calculations took 33 days on a dedicated Sun SPARC station-2, and Celenligil's et al. (1991b) 3-D calculation needed 35 CPU hours on CRAY-2. The NS

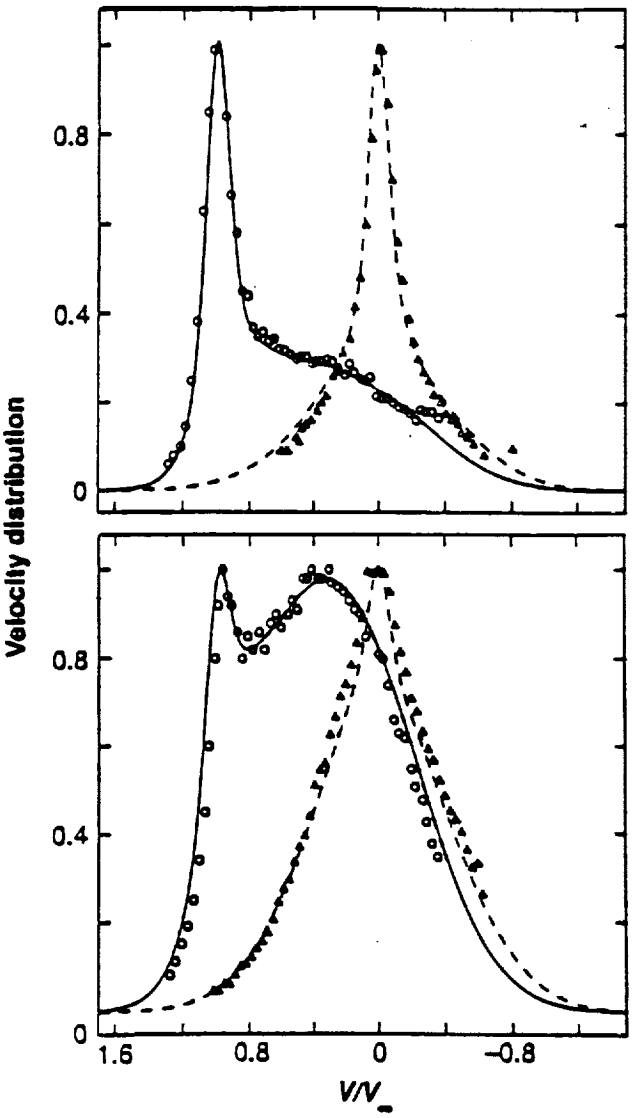

Fig. 13 Predicted and experimental velocity distributions (from Pham-Van-Diep et. al. 1989): (a) $\bar{n} = 0.285$, (b) $\bar{n} = 0.565$; experiment (symbols), DSMC parallel (solid curve), DSMC perpendicular (dashes).

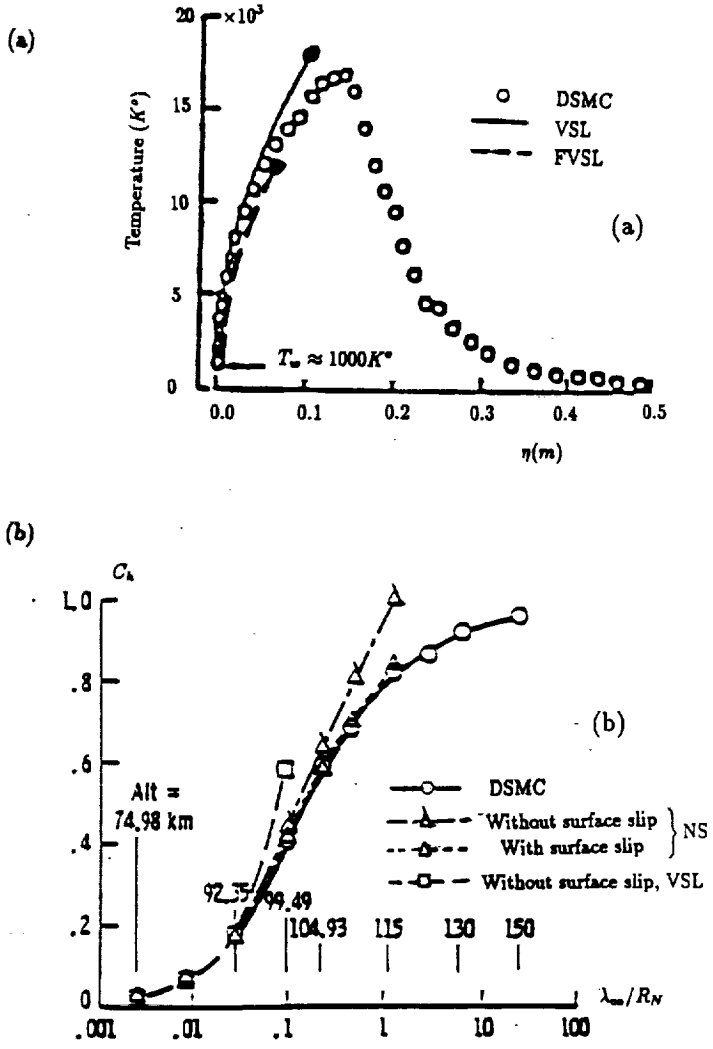

Fig. 14 Example comparing DSMC, VSL, FVSL, and NS calculations: (a) overal temperature distributions along stagnation streamline with $R_N = 1.3$m, $U_\infty = 7.5$km/sec., alt. 92km, $T_w \sim 1000°k$, non-catalytic surface; DSMC (open circle), VSL (solid curve), FVSL (dashes). [reproduced from Moss & Bird (1985)] (b) Surface heat-transfer coefficients as function of Knudsen number for $U_\infty = 7.2$ - 7.5km/sec., alt. 75 - 115km; DSMC (open circle), VSL without slip (squares), NS without slip (triangles with slashes), NS with slip (triangles) (reproduced from Gupta & Simmonds 1986).

based solutions/approximations have proven useful in low-density hypersonic flow studies (e.g. Cheng 1966) and compared reasonably well with surface heat flux measurements in hypersonic flows (Wittiliff & Wilson 1962, Vidal et al. 1963). With DSMC calculations, it becomes possible to assess the NS based results and other continuum extensions and identify their applicability domains. This was, in fact, accomplished by Moss & Bird (1985), Gupta & Simmonds (1986) Moss et al. (1987) and many subsequent workers, comparing DSMC, NS and NS-based viscous shock layer (VSL) calculations for the blunt nose region. Certain notions and concepts used in the subsequent discussions need to be clarified.

VISCOUS AND FULLY-VISCOUS SHOCK LAYERS Just as the inviscid shock layer in the classical theory, the concept of a *thin shock layer* is applicable to the viscous, heat-conducting flow region between the shock and the surface of a blunt/non-slender body, provided the density level there is much higher than that upstream. Viscous formulations based on thin-shock layer approximations could all be called viscous shock layer, but a distinction must be made between the version which use the viscous modified Rankine-Hugoniot relation at the outer boundary and that which assumes the inviscid shock relation. The latter version has been called the viscous shock layer (VSL) by Moss and coworkers, although being somewhat inconsistent in a strict sense. Thus the former version with the viscous modified shock condition will be referred to as the *fully* viscous shock layer (FVSL).

THE SHOCK SLIPS Owing to its resemblance to the wall slip, the change in the shock boundary conditions in the FVSL formulation, which includes corrections in tangential velocity and total enthalpy, has been called by Davis (1970), Moss and others "shock slips". Underlying these modified shock conditions is the stipulation that the density in the shock interior (structure) is low and comparable to the free-stream level; thus the tangential components of the mass, momentum and energy fluxes can little affect the balances in the normal flux components, as long as the thickness of the shock (structure) is small compared to the shock/body radius of curvature [even if the shock thickness becomes comparable to the thickness of the shock layer (Cheng 1961)]. This also implies that a shock-capturing NS solution should provide the shock slips correctly, even if the shock structure so obtained may not be physically correct on a kinetic-theory basis. The FVSL with the shock slips will provide a framework where a kinetic-theory base for the continuum extension can be found.

STRONG WALL COOLING AND WALL SLIPS A surface with low wall-to-stagnation temperature ratio ($T_w/T_o<<1$) is more of relevance to hypersonic flight than one with a nearly insulated wall; the strong cooling also makes the thin shock-layer analyses a better approximation for the FVSL, since the shock-layer density level is raised substantially through wall cooling. An additional consequence of strong wall cooling is in the limiting of the wall-slip influence on the FVSL and VSL, to a relative order of (Cheng 1966)

$$\sqrt{\epsilon \frac{T_w}{T_o}}$$

where ϵ in above is the small parameter in the shock-layer theory denoting the ratio of the free stream density to a typical shock-layer density.

COMPARISON OF NS-BASED AND DSMC CALCULATIONS To indicate the degree to, and the manner in which the NS-based predictions may differ from one another and from DSMC calculations in regime where departure from local translational equilibrium is significant, Figs. 14a,b, reproduce from Moss & Bird (1985) a comparison for temperature distribution along a stagnation streamline, and from Gupta & Simmond (1986) a comparison for the stagnation-point heat-transfer coefficient. The example of Fig. 14a has a strongly cooled noncatalytic nose with a 1.3 meter radius, at 7.5 km/sec speed, 92.4 km altitude. Here, Moss' NS-based VSL predictions (in solid lines) gives noticeably higher overall (effective) temperature than the DSMC data (in open circles) at the outer part of the

VLS; to indicate the shock-slip effect, a corresponding FVSL profile based on a binary reacting gas model (Cheng 1963) is also included as dashes; the viscous and heat-conduction corrections at the outer edge decrease the temperature in the outer portion of the FVSL and reduce its thickness. This figure serves to illustrate the great extent of the shock structure in this type of flow, which may be considered being almost twice the shock-layer thickness in this case. But owing to its lower density level, the influence on the downstream flow is limited. Figure 14b compares the heat-transfer coefficient C_H over a wide range of Knudsen numbers for a nose radius about 1.36 meter at speed 7.5 km/sec. Comparing with the DSMC results (in open circles), the VSL without wall slips and shock slips (in open squares) begins to depart at a Kn ~ 0.025, as Kn increases. The NS without wall slips (in open triangles) remains close to the main trend up to Kn ~ 0.25 where the shock slips are expected to be significant; this is consistent with the minor wall-slip effect (8.1) observed earlier. Surprisingly, the solution for NS with wall slips agrees with DSMC all the way up to Kn ~ 1. However, in a similar study by Lee et al. (1990), the NS with wall slips reaches the limit $C_H = 1$ at Kn ≈ 2.5 and suggests a peculiar trend of overshooting the limit at Kn ≥ 2.5.

8.5 On Kinetic-Theory Basis of NS, Burnett and Thirteen-Moment Equations

Early research on improvement of the NS description for rarefied flows by applying the Burnett (1936) and Grad's (1949) thirteen moment equations was not successful, and the general belief was that these higher-order equations from kinetic theory do not seem able to predict when the NS relations break down (see Schaaf & Chambré 1958, p. 718). This perception has apparently changed by recent studies with the help of modern CFD and with DSMC calculations, notably the study of the plane shock structure by Fiscko & Chapman (1988a,b).

SERIES EXPANSION NEAR CONTINUUM LIMIT The gas-kinetic base of the NS and Burnett equations is the formalism of the Chapman-Enskog expansion and the higher-order development of the velocity-distribution function for a *short* particle-collision time, λ/c or μ/p, compared to the flow characteristic time (Chapman & Cowling 1953, Vincenti & Kruger 1965, Kogan 1969, Ferziger & Kaper 1972).

THIRTEEN-MOMENT SYSTEM Grad's system of 13-moment equations is a particular set of moments of the Boltzmann equations--the Maxwell transfer equations, in which closure is achieved with the help of a form of the distribution function

$$f = \rho \left(\frac{\beta}{\pi}\right)^{3/2} e^{-\beta c^2}[1 + \mathbf{A}_{ij}c_i c_j + \mathbf{B}_i c_i + \mathbf{C}_i c^2 c_i] \tag{8.2a}$$

where $\beta = (2RT)^{-1}$, c_i is a thermal velocity component, $c^2 = c_1^2+c_2^2+c_3^2$, and the polynomial coefficients can be identified with stress-tensor components and heat fluxes as

$$\mathbf{A}_{ij} = \frac{p_{ij}}{2pRT}, \quad \mathbf{B}_i = -\frac{q_i}{pRT}, \quad \mathbf{C}_i = \frac{q_i}{pRT}\frac{c^2}{5RT}. \tag{8.2b}$$

The polynomial inside the square bracket came as a *truncated* Hermite polynomial expansion carried out for the twentieth moment in Grad's (1949) original work. Equation (8.2) is precisely the form for f needed in the Chapman-Enskog theory for the derivation of the NS and Fourier constitutive relations and the evaluation of the viscosity and heat-conductivity coefficients. Whereas, the p_{ij}, q_i, u_i and ρ are to be *solvewd* as unknowns in the PDE's of the 13-moment system, which does *not* require μ/p or $Kn = \lambda/L$ to be small as long as (8.2) remains adequate. This amounts to allowing nonvanishing

$$p_{i,j}/p, \; q_i/\sqrt{2RT} = O(1) \tag{8.3}$$

Interestingly, the full Burnett equations, including the boundary conditions for velocity and

temperature, are contained in (derivable from) Grad's 13-moment equations in the case of a Maxwell gas for asymptotically small μ/p or $|p_{ij}/p|$, even though Burnett's original theory involved a form far more complicated and of order higher than that in (8.2), as noted by Schaaf & Chambré (1958) and made more explicit by Yang (1992). The corrections for the non-Maxwell monatomic gas in both Burnett and 13-moment equations are rather small (Chapman & Cowling 1953, Fiscko & Chapman 1988; Chen, private communication).

BASIC ISSUES ON BURNETT AND 13-MOMENT EQUATIONS The Burnett equations as well as the extension to the Super-Burnett equations (Simon 1976) are valid only as successive corrections to the *Euler* equations for a nearly inviscid flow (outside of boundary and shear layers), inasmuch as inviscid/isentropic relations were used to simplified terms Dp_{ij}/Dt and Dq_i/Dt in the final form of the constitutive relations; it is not strictly applicable to either a fully viscous or boundary-layer region. This makes it more restrictive than merely requiring $|p_{ij}/p|$ being small. More critical is the unresolved issue with the proper boundary conditions when the Burnett system is solved as full equations without further approximations for $Kn \neq 0$. As Schaaf & Chambré (1958) noted, at the Burnett level, terms of an order higher in derivatie occur in each equation and an additional boundary condition must be prescribed. Thus a *nonuniqueness* problem will arise unless the system possesses a special property for the exception. The issue cannot be settled by simply demonstrating the existence of a solution.

For application to supersonic flows, Grad's 13-moment equations fail to yield a normal shock structure at Mach number exceeding 1.65, as is well known (Grad 1952). The system without modification cannot provide a base for the analysis of the entire flow field which include the shock structure. The discussion in §8.7 will examine its applicability to the study of flow behind shock.

8.6 Burnett Equations as CFD Model for Rarefied Hypersonic Flows

NS calculations have been known to give poor shock-structure descriptions when compared to particle-simulation and experimental results (Schaaf & Chambré 1958, Bird 1978, Muntz 1989). Using flux-splitting technique, Fiscko & Chapman (1988a,b) found that Burnett equations provide much greater accuracy than NS equations for 1-D shock structure in a monatomic gas, although its degree of improvement over NS varies, depending on the Mach number and the viscosity-temperature law of the gas, and on the flow quantities of interest. Figure 15 reproduces from Fiscko & Chapman (1988a) a comparison of the inverse density thicknesses (IDT) for an argon shock predicted by Burnett equations (in solid curves), NS equations (in fine dots) and DSMC (in open circles) over a wide range of Mach numbers (cf. Muntz 1989 for definition of IDT). The encouraging agreement with the particle-simulation results suggests that a CFD model based on the Burnett equations may provide a much improved *shock-capturing* capability in a rarefied hypersonic flow where a realistic description of the shock structure at high temperature is of vital aerothermodynamic interest. Apart from the issue on the surface boundary conditions, there is another obstacle to this extension, noted and resolved by Zhong et al. (1991). Namely, the numerical solution is linearly unstable to disturbances with wave length comparable, or less than, the mean free path (Bobylev 1982, Foch 1973), and this difficulty was believed to place a handicap on Fiscko's earlier calculations; it would also pose a computation problem if one desires to study the higher altitude effects for the same body geometry using a *fixed* grid. Zhong et al. overcame this problem by adding *several* higher-order derivative terms to the Burnett constitutive equations. These added terms have forms similar to certain terms at the Super-Burnett level but with different coefficients (and signs). The *augmented* Burnett constitutive equations/relations for the deviatorial stress and heat-flux components are written as

$$\sigma_{ij} = \sigma_{ij}^{(1)}+\sigma_{ij}^{(2)}+\sigma_{ij}^{(a)}, \qquad q_i = q_i^{(1)}+q_i^{(2)}+q_i^{(a)}$$

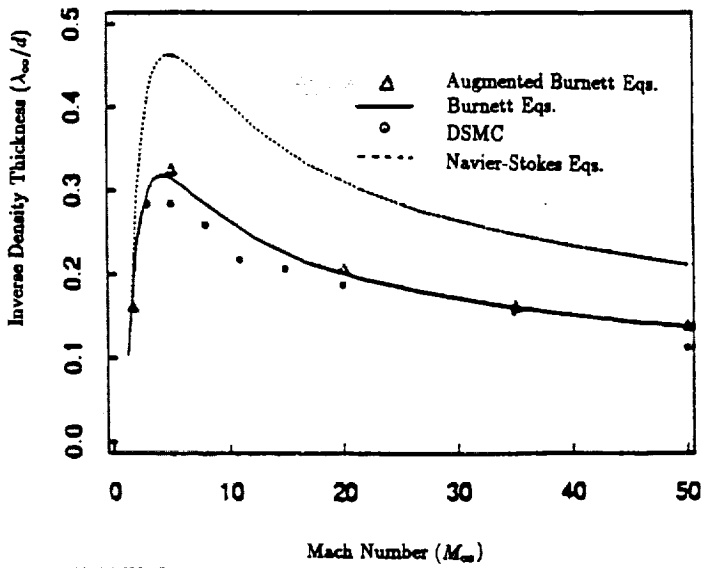

Fig. 15 Comparison of Navier-Stokes (dots), Burnett (solid curve), Stabilized Burnett (triangles), and DSMC (circles) calculations in inverse density-thickness ratio at different Mach numbers (reproduced from Fiscko & Chapman 1988 a,b, also Zhong et. al. 1991).

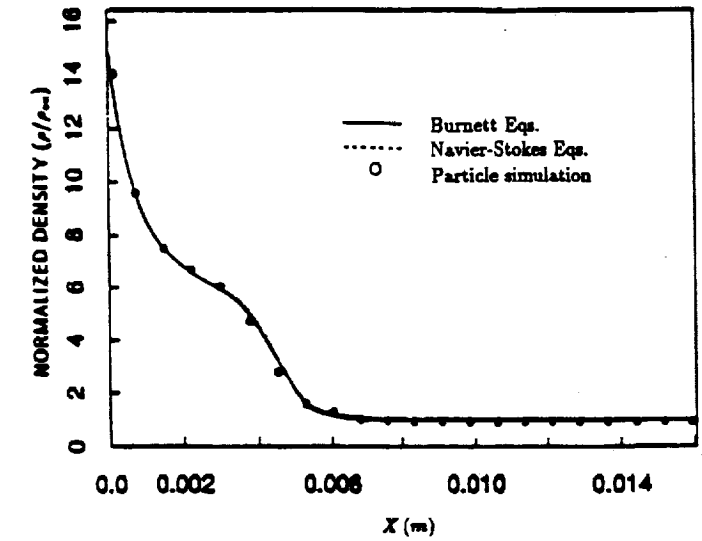

(a)

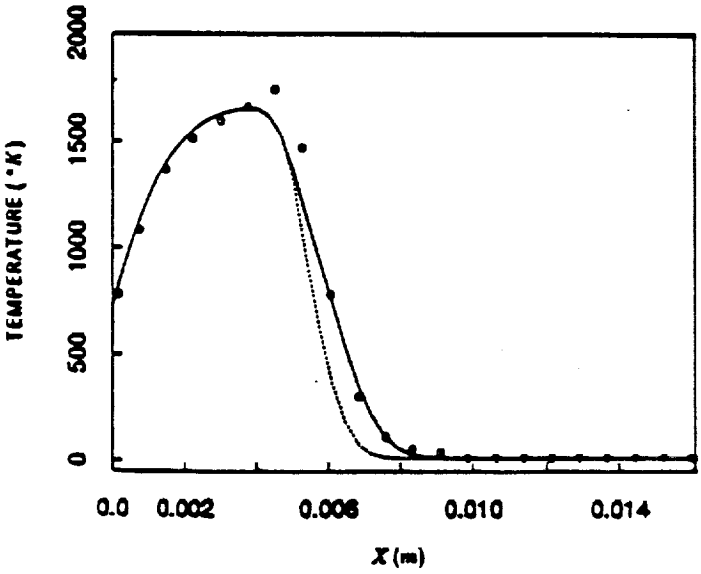

(b)

Fig. 16 Comparison of stabilized Burnett, Navier-Stokes and particle simulation calculations along stagnation streamline for case IV ($M_\infty = 25, \alpha = 30°, K_n = 0.28; K^2 = 0.95$): (a) density (b) translational temperature. (reproduced from Zhong et al. 1991)

where supercripts (1) and (2) refer to the NS and Burnett levels, respectively, and (a) indicates the added terms. In the 1-D case, for example, $\sigma_{11}^{(2)}$ and $q_1^{(2)}$ contain terms like

$$\sigma_{11}^2 = \frac{\mu^2}{p}\left(\alpha_1 u_x^2 + \alpha_7 RT_{xx} + \alpha_9 \frac{RT}{\rho}\rho_{xx} + \cdots\right)$$
$$q_1^{(2)} = \frac{\mu^2}{p}\left(\gamma_1 \frac{T_x u_x}{T} + \gamma_3 u_{xx} + \cdots\right) \tag{8.4a}$$

and the added terms are

$$\sigma_{11}^{(a)} = \frac{\mu^3}{p^2}\omega_7 RT u_{xxx}$$
$$q_1^{(a)} = \frac{\mu^3}{p\rho}\left[\theta_7 RT_{xxx} + \theta_6 \frac{RT}{\rho}\rho_{xxx}\right] \tag{8.4b}$$

The set $\omega_7 = 2/9$, $\theta_6 = -5/8$ and $\theta_7 = 11/16$, which is by no means the unique choice, proves to make the linearized Burnett equations stable. Incidentally, this set turns out to be precisely that given by Wang-Chang (1948) for a Maxwell gas, of which the θ_7 value did not agree with the correct value -157/116. The augmented Burnett results enjoy a much higher accuracy than Fiscko's earlier version and are marked also in Fig. 15 as open triangles.

More interesting are perhaps the 2-D examples in Zhong et al. (1991) which compares the NS, augmented Burnett, and particle-simulation calculations. They are among the first Burnett solutions to hypersonic blunt-body problems to appear, and to which the boundary-condition issues must be addressed. The (M_∞,Kn) pairs considered in the four cases are ($4{,}067\times10^{-4}$)(10,0.10)(10,1.2) and (25,0.28), referred to as cases I, II, III and IV, respectively. A constant specific heat ratio $\gamma = 1.40$ was assumed, except in case IV where rotational relaxation is allowed in both Burnett and the particle simulations; whether the relaxation models can be identified to those in Lumpkin & Chapman (1991) and Lumpkin et al. (1989) is unclear. For these examples, the surface temperature is not low, being in the range $T_w/T_o \sim 1/3 - 1/2$. Here, the Burnett and NS solutions shared the *same* slip boundary conditions, while the corresponding surface conditions for the particle simulation calculation was not explained. Of interest are the density and temperature distributions along the stagnation streamline in cases II, III and IV where the differences among the three solution sets are surprisingly small, especially in the density profiles. Even in the thick shock interior, where discrepancies of the NS temperature predictions are noticeable, the NS solution actually describes the temperature profile not so poorly.

Figure 16 reproduced from Zhong et al. (1991) compares the density and temperature for case IV. Of vital engineering interest is that temperature profiles of the three solutions sets become *indistinguishable* from one another downstream of the shock structure in all cases. This is rather surprising, not only because NS results have never before been shown being in agreement so well with Burnett and particle simulation in the shock interior, but also because the FVSL parameter K^2 (Cheng 1966, see below) is of unit order or smaller in cases II-IV, which signifies large departures from translational equilibrium. These could have resulted from the Sutherland viscosity law assumed or from the particular iterative procedure used which avoid the additional boundary conditions by extrpolating from the interior; it remains to be further examined. While the study shows Burnett equations can yield a solution closely matched the particle-simulation results, the same study also indicates that NS calculations can predict the shock and flow structures almost as well as the Burnetts. This interesting CFD work falls short in settling the obvious uniqueness issue which cannot be answered by simply demonstrating the solution's existence, as noted earlier. For the steady Couette flow problem, Lee (private communication) shows that, even with the extrapolation technique, the

solution is not unique and depends on the initial input for the iteration.

8.7 Thirteen-Moment Equations as Basis for Viscous Shock Layer Theory

NEED OF GAS KINETIC BASIS As noted earlier, the use of FVSL, VSL as well as the full NS equations in rarefied hypersonic flow analyses anticipates the viscous and other molecular transport effects to rank equally with the convective processes, which also implies condition (8.3). The very same condition indicates, however, a large departure from the translational equilibrium, invalidating the gas-kinetic base for the NS and the Burnett equations. Grad's 13-moment theory, which allows condition (8.3), may therefore serve a kinetic-theory base for viscous shock-layer anslyses. Another reason for using the 13-moment equations is the absence of ambiguity in the type and number of admissible boundary conditions on a body surface. By considering the number of characteristics reaching the boundary, Grad (1949) showed that the number and type in question are the same as in NS; this can be confirmed by examining the nature of the 13-moment equations in a Couette flow [Cheng et al. 1989, Eq. (4.35)]. Using scales typical of the flow in a shock layer, it is possible to express the order of magnitude of $|p_{ij}/p|$ more explicitly in the form of the *reciprocal* of a local Reynolds number

$$\bar{x} = \epsilon \frac{\rho_\infty U_\infty x}{\mu_o} \left(\frac{\mu_o}{\mu_*} \frac{T_*}{T_o} \right) sec\beta^* \tag{8.5}$$

where β_* is the shock or body incidence angle, the subscripts "$*$" refer to a suitable reference condition and x is a distance or reference length. With x replaced by the nose radius R_N, $\bar{x}$ is identified with the K^2 in Cheng's (1961,1963,1964) early NS-based theory. Thus $\bar{x}$ or K^2 directly control both the shock slip and departure from translational equilibrium. The Knudsen number $Kn \equiv \lambda_\infty/L$ and the $V \equiv \chi/M_\infty{}^2$ commonly used in rarefied gas dynamics are related to $\bar{x}$ as

$$Kn \sim 2 \left(\epsilon \frac{T_*}{T_o} \right)^{1/2} (\bar{x})^{-1}, \quad \bar{V} \sim (\bar{x} cos\beta)^{-1/2} \tag{8.6}$$

THE THIN-LAYER APPROXIMATION AND QUASI-1-D SHOCK STRUCTURE Using scales appropriate to the shock structure, thin-layer approximations can be applied to derive the equations governing the quasi-1-D shock structure. They can be integrated to arrive at the modified Rankine-Hugoniot relation allowing the shear-stress and heat-flux contributions immediately behind the shock, identified as the "shock slips". Using conventional notations in the shock-layer theory, with y and v referring to the coordinate and velocity component in the direction normal to the body surface. The latter conditions read

$$u - u_\infty = p_{12}/m_1, \qquad w - w_1 = p_{32}/m_1 \tag{8.7}$$

$$H - H_\infty = (up_{12} + wp_{32} + q_2)/m_1$$

where $m_1 = \rho_\infty v_1$ is the component of free-stream velocity normal to the surface, q_2 is the normal heat flux component, p_{12} and p_{32} are pressure tensor components associated with (x,y) and (z,y) respectively. Subject to error of order ϵ, this provides the outer boundary conditions for the shock-layer flow, irrespective of the gas-kinetic model in the shock interior (Cheng et al. 1991). The remaining shock condition is $P_{22} = m_1 v_1$, where the normal pressure-tensor component P_{22} is not the thermodynamic pressure p, owing to translational noequilibrium.

FVSL BASED ON 13-MOMENT EQUATIONS The governing equations for the shock layer are, to the leading order, essentially the same as in viscous shock-layer theories, except that constitutive relations expressing p_{12}, p_{32}, p_{22} and q_2 in terms of flow gradients must now be replaced by the 13-moment

leading order, essentially the same as in viscous shock-layer theories, except that constitutive relations expressing p_{12}, p_{32}, p_{22} and q_2 in terms of flow gradients must now be replaced by the 13-moment theory. Under the thin-layer approximation and with the formalism of a small ε familiar from the shock-layer theory, i.e., considering R/C_p being small, the constitutive relations in question can be reduced simply to (Cheng et al. 1989, 1991)

$$p_{12} = -\frac{P_{22}}{p}\mu\frac{\partial u}{\partial y}, \qquad p_{32} = -\frac{P_{22}}{p}\mu\frac{\partial w}{\partial y} \tag{8.8a,b}$$

$$q_2 = -\frac{P_{22}}{p}k\frac{\partial T}{\partial y} \tag{8.8c}$$

$$\frac{p}{P_{22}} = 1 + \frac{2}{3}\left(\frac{\mu}{p}\frac{\partial u}{\partial y}\right)^2 + \frac{2}{3}\left(\frac{\mu}{p}\frac{\partial w}{\partial y}\right)^2 - \frac{4}{3}\frac{R}{P_r}\frac{1}{P_{22}}\frac{\mu}{p}\frac{\partial}{\partial y}P_{22}\frac{\mu}{p}\frac{\partial T}{\partial y} \tag{8.8d}$$

The above expressions differ from the corresponding NS based relations mainly in the appearance of the *common factor* P_{22}/p to be determined through a nonlinear relation to the velocity and temperature gradients (8.8d). It is, in fact, through the p, not P_{22}, that translational nonequilibrium will affect the dynamics and thermodynamics of a viscous shock layer. Except for the last equation, the above constitutive relations involve derivatives of u and T no higher than the *first* order and differ from those in the Burnett theory. We note that the last (8.8d) is a thermal stress (Kogan 1969) and is formally a higher order term, but is included for its exceptionally large coefficient and physical significance. To complete the formulation, we may apply wall-slip equations from Grad's wall model suitably simplified in a manner consistent with (8.7)-(8.8). These wall-slip effects, however, can influence the shock-layer flow at the most of relative order $(\varepsilon T_w/T_o)^{1/2}$ as indicated earlier. They have been demonstrated to be negligibly small even for exceptionally large accommodation coefficients (Cheng & Wong 1988).

The observation made above on the nonequilibrium influence through the ratio P_{22}/p indicates the possibility of successfully correlating a kinetic-based shock-layer flow with a NS-based flow. Its key lies in the recognition that the reciprocal of the density ρ or p always appears in a product together with normal derivative $\partial/\partial y$ both in the governing PDE's and in the outer boundary conditions involving the shock slips. The ε or p may then be eliminated in this case by the use of Dorodnitsyn or von Mises variables, through which the governing equation system is transformed to a NS-based system, with slightly different wall-slip boundary conditions. The latter is inconsequential for the strongly cooled surface of interest. This *correlation principle* holds for the tangential velocity components and the enthalpy, and also for the major stress components and the heat flux. A consequence is that the skin friction and surface heating rate are predictable from the NS-based equations, being unaffected by the translational nonequilibrium to the leading order, although the streamline pattern and shock-layer thickness will be accordingly displaced. The present version of the theory therefore provides a kinetic-theory base for explaining the good agreement of the NS-based FVSL analyses with early heat-transfer measurements.

FLAT PLATE AT INCIDENCE: CORRELATING DSMC AND NS-BASED CALCULATIONS The flow about a flat plate at 40° attack angle was studied by Cheng et al. (1989,1990,1991), and also Cheng (1989), as a generic lifting surface problem in rarefied hypersonic flow, for which FVSL, parabolized (thin-layer) NS, and time-accurate NS calculations were made and compared to corresponding DSMC

computations (Dogra & Moss 1989, Dogra et al. 1989) and examples include (monatomic) Maxwell gas and diatomic-gas model with $\gamma = 1.40$ and $Pr = 0.72$ (which implies a fast rotation-translation energy transfer), and cases with different viscosity-temperature relations, wall temperatures, and wall-slip models. While some of the DSMC data were generated from a code which allows internal excitation and chemical reaction of a model air, the latter effects on aerothermodynamics are negligible even at flow speed of 7.5 km/sec, owing to the high degree of gas rarefaction at altitudes 90-130 km. The coefficients of heat transfer and skin friction, C_H and C_f, from three sets of DSMC data and six sets of NS-based results, each with different M_∞, Re and viscosity law were determined over a wide range of $\bar{x}$, 0.2-10 ($\bar{x} = 10^{-3}$-10, if the DSMC data near the collision-free limit is also included). Figure 17 presents the correlation/comparison in C_H as function of $\bar{x}$; even though a perfect Reynolds analogy is not expected, the corresponding correlation for C_f in this case turns out to be almost indistinguishable from that in Fig. 17 (except a portion of DSMC calculation for the 100 km altitude which defies explanation)

The lift-to-drag ratio of the plate at 40° incidence computed from the integrated normal and tangential forces on the windward side are reproduced from Cheng et al. (1991) as a function of $\bar{x}$ in solid curves, which agrees exceedingly well with Dogra et al. (1989) DSMC calculation for a one-meter plate (in open circles with slashes) over the entire $\bar{x}$-range (2×10^{-2} through 15). Also included as a solid curve is the L/D computed for a plate at 20° attack angle. Of interest are L/D values computed for ten widely different planforms based on the 2-D distributions of skin friction and normal force (reproduced from Cheng (1991). These calculations (Hoover et al. 1992) used a version of the strip method which is the result of the 3-D FVSL theory for a flat-bottom surface (Cheng et al. 1991). When the distance x in the 2-D problem were taken to be the *span-averaged* chord (SAC), the ten L/D values fall into the vicinity of the strictly 2-D results. This is surprising, because as altitude or Knudsen number increases, the planform dimension and shape are expected to strongly affect the skin friction hence the L/D. This insensitivity of the L/D on planform indicates a way to identify the *bridging function* for planar lifting surface (Warr 1970, Wilhite et al. 1985, Potter 1988), which is provided here by the 2-D data for an inclined plate.

The flows over an aligned flat plate and on the lee side of a flat surface remain as examples for which still more can be learned from critical examination of the continuun-extension and particle simulation calculations.

9. CONCLUDING REMARKS

In this article, an attempt has been made to reflect on current focuses in certain areas of hypersonic flow research by examining the recent works and their issues. The study addresses aspects of viscous interaction, flow instability, and nonequilibrium aerothermodynamics pertaining to theoretical interest. The field is a diverse one, and many exciting works may have either escaped the writer's notice or been abandoned for the sake of space. As noted in the text, students of hypersonic viscous flow must face the *transition* problems towards the two opposite ends of the Reynolds or Knudsen number range (§§5,8), which represents two regimes where unresolved fluid/gas dynamic problems abound. Central to the hypersonic flow studies is high-temperature physical gas dynamics (§6); here, a number of issues on modelling the intermolecular potentials and inelastic collisions remain the obstacles to quantitative predictions. Research in combustion and scramjet propulsion will certainly be benefitted by advances in turbulent mixing and new CFD strategies on multi-scaled complex reactions.

Apart from many omissions, the view and interest expressed by the author has been limited to the

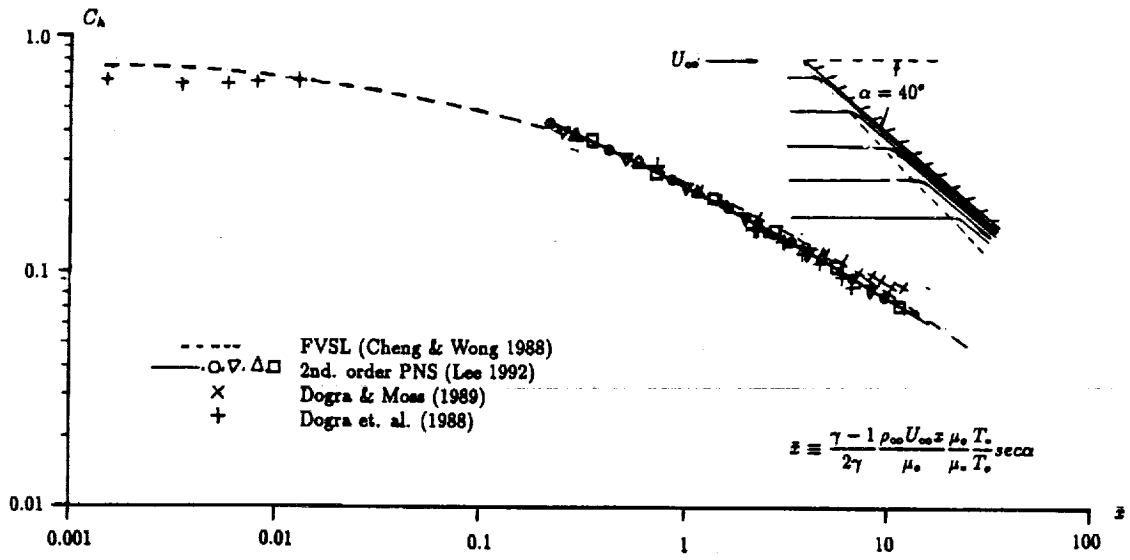

fig. 17 Correlation of DSMC and NS-based calculations with FVSL analysis for surface-heating rate as function of a rescaled Reynolds number $\bar{x}$ on the compression side of a strongly cooled ($T_w/T_o \approx 0.04$) flat surface at 40° attack angle, speed 7.5km/sec. in a standard atmosphere.

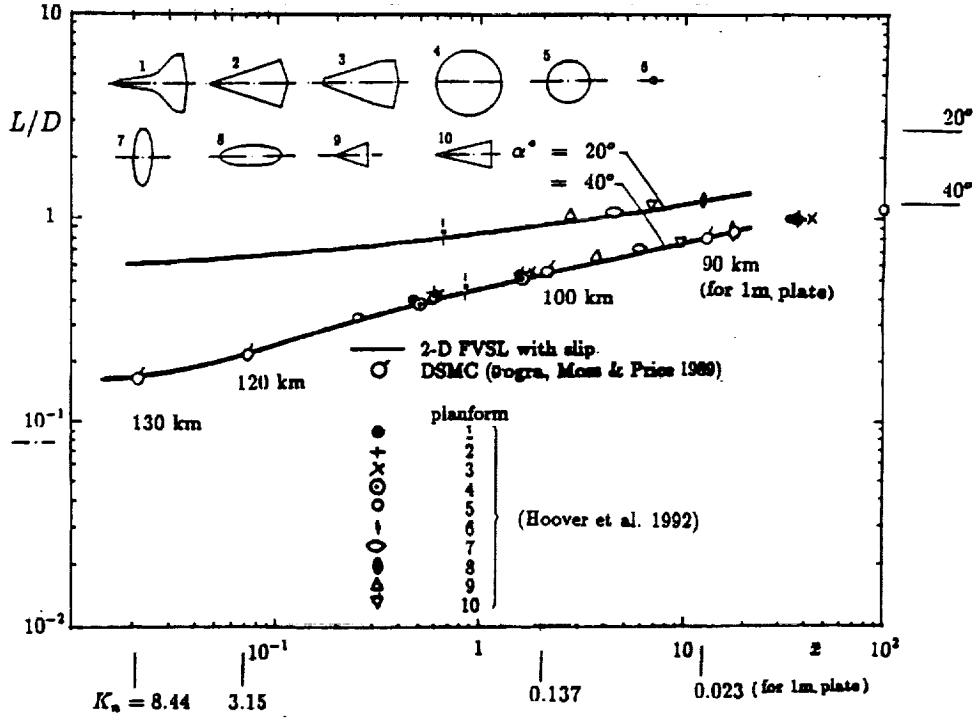

Fig. 18 Correlation of lift-to-drag ratio of planar lifting surfaces at 40° attack angle in a standard atmosphere with 2-D, DSMC and FVSL results as a function of $\bar{x}$. The data in symbols for 10 planforms were computed from a strip method based on 3-D FVSL theory. SAC means the span-averaged chord and varies among Planforms 1-10 from 0.47 through 19.19 meters.

theorectical side. However, even for the sake of theoretical development, the lack of pertinent experimental data in the right energy and density ranges is believed to be among the major obstacles to progress in aerothermodynamic research for hypersonic flight. Flight experiments performed by Space-Shuttle missions and the AFE Program referred to often in the text have been extremely valuable. To enable laboratory simulation of nonequilibrium effects anticipated for transatmospheric flight, facilities capable to generate high enthalpy flow at density levels higher than in existing laboratories are needed (Hornung 1988). A new free-piston shock tunnel capable to realize a test-section stagnation temperature of $10^5 K^\circ$ at Reynolds number 50×10^6/cm are being completed and preliminary tests has begun (H. Hornung et al. 1992). Another laboratory study worthy of note as well as theoretical support is the nonequilibrium flow experiment of iodine vapor which has low activation energies for vibrational excitation and dissociation, and can be studied in a laboratory with modest resources (Pham-Van-Diep et al. 1992).

ACKNOWLEDGEMENTS

This study has been supported by the NASA/DOD Grant NAGW-1061 and by AFOSR Math Information Science Program. Many individuals have helped the author in one way or another during the course of this review study, among them are S.N Brown, D. Bushnell, J.A. Domaradzki, D.A. Erwin, M.M. Hafez, J.A. Kunc, C.J. Lee, R.E. Melnik, J.N. Moss, E.P. Muntz, C. Park, C.E. Treanor, P.L. Varghese, H.T. Yang, and X.L. Zhong; also to be thanked are T. Austin, Y. Bao, C. Holguin, D. Wadsworth, D. Weaver and E.Y. Wong for their invaluable assistance.

REFERENCES

Allen, R.A., Rose, P.H., Camm, J.C. 1962. *AVCO-Everett Res. Lab. Research Report 156*

Anderson, D.A., Tannehill, J.C., Pletcher, R.H. 1984. *Computational Fluid Mechanics and Heat Transfer*, Hemisphere Pub. Corp.

Anderson, J.D., Jr. 1989. *Hypersonic and High Temperature Gas Dynamics*, N.Y. McGraw Hill

Anderson, J.D., Chang, J., McLaughlin, T.A. 1992. *AIAA paper 92-0302*

Anderson, J.D., Ferguson, Lewis, M.J. 1991. *AIAA paper 91-0530*

Anderson, J.D., Lewis, M.J., Corda, S., Blankson, I.M. (ed.) 1990. *Proc. 1st Inter. Hypersonic Waverider Symp.*, Univ. Maryland, Oct. 17-19, 1990; to appear as *AIAA prog. in Astro. Aero. Series*

Baganoff, D., McDonald, J.D. 1990. *Phys. Fluid A* 2: 1248-1259

Baldwin, B.S., Lomax, H. 1978. *AIAA paper 78-257*

Balsa, T.F., Goldstein, M.E. 1990. *J. Fluid Mech. 216*: 598-

Beam, R., Warming, R.F. 1978. *AIAA J. 16: 393-402*

Beckwith, I.E., Holley, B.B., 1981. *NASA TP-1869*

Beylich, A.E., ed. 1991. *Rarefied Gas Dynamics*, Proc. 17th Inter. Symp., Aachen, VCH Verlag

Billig, F.S. 1992. *AIAA paper 92-0001*

Bird, G.A. 1976. *Molecular Gas Dynamics*, Clarendon Press, Oxford

Bird, G.A. 1978. *Ann. Rev. Fluid Mech. 10*: 11-31

Bird, G.A. 1979. *Rarefied Gas Dynamics 11*: 365-388

Bird, G.A. 1985. *AIAA paper 85-0994*

Bird, G.A. 1987. *AIAA paper 87-1543*

Bird, G.A. 1989. *Rarefied Gas Dynamics 16*:

Bird, G.A. 1990a. *AIAA paper 90-1962*

Bird, G.A. 1990b. *The F9 Program System User's Manual*, G.A.B Consulting, Ply. Ltd.

Blackaby, N.D., Cowley, S.J., Hall, P. 1992. (Submitted to *J. Fluid Mech.*, private communication)

Blottner, F.G. 1990. *J. Spacecraft and Rockets, 27*: 113-122

Bobylev, A.V. 1982. *Soc. Phys. Dokl. 27* (1)

Borgnakke, C., Larsen, P.S. 1975. *J. Computational Physics 18*: 405-420

Bowcutt, K.G., Anderson, J.D., Capriotti, D. 1987. *AIAA paper 87-0272*

Boyd, I.D. 1990. *Phys. Fluids* A *2* 447 (1990)

Boyd, I.D. 1991. *Phys. Fluids A 3* (7): 1785-1791

Boyd, I.D. 1992. submitted to *J. Computational Physics*:

Boyd, I.D., Penko, P.F., Meissner, D.L. 1991. *AIAA paper 91-1363*

Brown, S.N., Cheng, H.K. Lee, C.J. 1990. *J. Fluid Mech., 220* : 309-337

Brown, S.N., Khorrami, A.F., Neish, A., Smith, F.T. 1991. *Phil. Trans. R. Soc. Lond. A 335*: 139-152

Brown, S.N., Stewartson, K.S. 1975. *Quart. J. Mech. Appl. Math., 28*: 75-

Brown, S.N., Stewartson, K.S., Williams, P.G. 1975. *Phys. Fluids 18*: 633-

Burggraf, O.R., Rizzetta, D. Werle, M.J., Vasta, V.N. 1979. *1979 AIAA J. 17*: 336-343

Burns, B.R. 1989. *Proc. Inter. Conf. Hypersonic Aerodynamics*: paper no. 1

Burnett, D. 1936. *Proc. London Math. Soc.* Ser. 2 *40*, no. 3: 382-435

Bush, W.B. 1966. *J. Fluid Mech. 25*: 51-64

Bush, W.B., Cross, A.K. *J. Fluid Mech. 29*: 349-359

Butta, B.A., Lewis, C.H. 1990. *J. Spacecraft and Rockets, 27* : 194-204

Campbell, D.H. 1991. *AIAA paper 91-1362*

Candler, G.V. 1990. *AIAA paper 90-1695*

Candler, G.V. MacCormack, R.N. 1988. *AIAA paper 88-0511*

Carlson, A.B., Hassan, H.A. 1991. *AIAA paper 91-1409*

Carlson, A.B., Wilmoth, R.G. 1992. *AIAA paper 92-0492*

Cauchon. D.L. 1966. *NASA TM X-1402*

Cebeci, T., Bradshaw, P. 1988. *Physical and Computational Aspects of Convective Heat Transfer*, Spring Verlag

Celenligil, M.C. Moss, J.N. 1991. *AIAA paper 91-1315*

Celenligil, M.C. Moss, J.N., Blachard, R.C. 1991. *AIAA J. 29*: 52-27

Chapman, D.R. 1992. *Aerospace America* Jan. 16-59

Chapman, S., Cowling, T.G. 1953. *The Mathematical Theory of Nonuniform Gases*, Cambridge Univ. Press

Cheng, H.K. 1961. *Proc. Heat Transfer and Fluid Mech. Inst.*, ed. R.C. Bender et al, Stanford Univ. Press: 161-175

Cheng, H.K. 1963. *Cornell Aero. Lab. Report AF-1285-A-10*

Cheng, H.K. 1966. *Fundamental Phenomena in Hypersonic Flow*, ed. G.J. Hall, Cornell Univ. Press: 91-132

Cheng, H.K. 1989. *Proc. Inter. hypersonic Aerodynamics*, Univ. manchester, Manchester, England

Cheng, H.K. 1990. (Book Review) *AIAA J, 28*: 766-768

Cheng, H.K. 1991. *Proc. 4th Inter. Symp. Comp. Fluid Dynamics* Davis, Ca.

Cheng, H.K., Lee, C.J., Wong, E.Y., Yang, H.T. 1989. *AIAA paper 89-1663*

Cheng, H.K., Wong, E.Y. 1988. Univ. So. Calif. Dept. Aerospace Eng. Report *USCAE 147*

Cheng, H.K., Wong, E.Y., Dogra, V.K. 1991. *AIAA paper 91-0783*

Cheng, H.K., Wong, E.Y., Hoover, L.N., Dogra, V.K. 1990. *Proc. 1st Inter. Hypersonic Waverider Symp.* Univ. Maryland, Md

Cheng, S.I. 1989. *Proc. Energy Combust. Sci. 15*: 183-202

Cheung, S., Cheer A., Hafez, M., Flores, J. 1991. *AIAA J. 29*: 1214-1223

Chuck, C., Eberhardt, S., Pratt, D.T. 1991. *AIAA paper 91-1674*

Chung, C.H., DeWitt, K.J., Jeng, D.R. 1991. *AIAA paper 91-1343*

Clarke, J.F., McChestney, M. 1964. *The Dynamics of Real Gases*, Butterworths

Cloakley, T.J. 1983. *AIAA paper 83-1693*

Corda, S., Anderson, J.D., Jr. 1988. *AIAA paper 88-0369*

Cowley, S.J., Hall, P. 1990. *J. Fluid Mech. 214*: 17-42

Cox, R.N., Crabtree, L.F. 1965. *Elements of Hypersonic Aerodynamics*, English Univ. Press

Davis, R.T. 1970. *AIAA J. 8*: 843-851

Demetriades, A. 1978. *Proc. Heat Transfer Fluid Mech. Inst.* : 39-54; also *AIAA paper 74-535* (1974)

Dogra, V.K., Moss, J.N. 1989. *AIAA paper 89-1712*

Dogra, V.K., Moss, J.N., Price, J.M. 1989. *Rarefied Gas Dynamics* (ed. E.P. Muntz et. al.) *AIAA Conf. Seris*, Acad. Press.

Dogra, V.K., Moss, J.N., Wilmoth, R.G., Price, J.M. 1992. *AIAA paper 92-0495*

Dogun, L. 1991. *AIAA paper 91-1365*

Eckland, D.R., Northam, G.B. 1992. *AIAA paper 92-0624*

Edney, B. 1968. *Aeron. Res. Inst. Sweden, Stockholm, Rept. 115*; also *AIAA J. 6*, 15-21

Edwards, T.A., Flores, J. 1990. *J. Spacecraft & Rocket 27*: 123-130

Eggers, A.J., Ashley, H., Springer, G. 1990. *Proc. 1st. Inter. Hypersonic Waverider Sypm.*, Univ. Maryland, College park, Md., Oct. 17-19, 1990

Erwin, D.A., Pham-Van-Diep, G.C., Muntz, E.P. 1991. *Phys. Fulids A 3*: 697-705

Ferri, A. 1973. *Annual Rev. Fluid Mechanics 3*: 301-338

Ferziger, J.H., Kaper, H.G. 1972. *Math. Theory of Transport Processes in Gases*, North-Holland pub. Co.

Fiscko, K.A., Chapman, D.R. 1988a. *AIAA paper 88-2733*

Fiscko, K.A., Chapman, D.R. 1988b. *Rarefied Gas Dynamics*, Proc. 16th Inter. Symp. R.G.D.

Foch, J.D. 1973. *Acta Physical Austriaca, Suppl. X*: 123-140

Furlani, T.R., Lordi, J. 1989. *AIAA paper 89-1667*

Gajjar, J., Smith, F.T. 1983 *Mathematica, 30*:77-93

Gibson, W.E., Marrone, P.V. 1962. *Phys. Fluids 5*: 1649-1656

Glass, C.E., Weiting, A.R., Holden, M.S. 1989. *NASP TN 1085*

Gnoffo, P.A. 1989. *AIAA paper 89-1972*

Gnoffo, P.A. 1990. *J. Spacecraft and Rockets, 27*: 131-142

Goldstein, M.E., Wundrow, D.W. 1990. *J. Fluid Mech. 219*: 585-607

Gonzales, D.A., Varghese, P.L. 1991. *AIAA paper 91-1370*

Gonzales, D.A., Varghese, P.L. 1992. *AIAA paper 92-0808*

Goussis, D.A., Lam, S.H., Gnoffo, P.A. 1990. *AIAA paper 90-0644*

Grad, H. 1949. *Comm. Pure Appl. Math. 2*, no. 4: 331-407

Grad, H. 1952. *Comm. Pure Appl. Math. 5*, no. 3: 257-300

Greendyke, R.B., Gnoffo, P.A., Lawrence, R.W. 1992. *AIAA paper 92-0804*

Gupta, R.N. 1987. *AIAA paper 87-1576*

Gupta, R.N., Simmonds, A.L. 1986. *AIAA paper 86-1349*

Gupta, R.N., Lee, K.P., Moss, J.N., Sutton, K. 1990. *AIAA paper 90-1697*

Gupta, R.N., Lee, K.P., Moss, J.N., Sutton, K. 1991. *AIAA paper 91-1345*

Gupta, R.N., Lee, K.P., Zoby, E.V. 1992. *AIAA paper 92-2897*

Hall, J.G., Eschenroeder, A.A., Marrone, P.V. 1962. *J. Aerospace Sci., 29*: 1038-1051

Hamilton, H.H., Gupta, R.N., Jones,J.J. 1991. *J. Spacecraft & Rocket 28*:125-128

Hansen, C.F. 1990. *Final Report on NASA Grant NAG1-1046*

Harten, A. 1983. *J. Comp. Phys 49*: 357-393

Hartung, L.C. 1991. *AIAA paper 91-1406*

Hartung, L.C., Mitcheltree, R.A., Gnoffo, P.A. 1991. *AIAA paper 91-0571*

Harvey, J.K., Celenligil, M.C., Dominy, R.G., Gilmore, M.G. 1989. *AIAA paper 89-1709*

Hayes, W.D., Probstein, R.F. 1959. *Hypersonic Flow Theory*, Academic Press

Herbert, Th. 1988. *Ann. Rev. Fluid Mech. 20*: 487-526

Hertzberg, A., Bruckner, A.P., Bogdanoff, D.W. 1988. *AIAA J. 26*:195-203

Hertzberg, A., Bruckner, A.P., Knowlen, C . 1991. *Shock Waves 1*:17-25

Ho, C.M., Gutmark, E. 1987. *J. Fluid Mech., 179*: 385-405

Hoffman, K.A. 1989. *Computational Fluid Dynamics for Engineers* Engineering Education System™, Austin, Tx

Holden, M. Moselle, J.R. 1969. *CALSPAN Report AF-2410-A-1*

Holden, M., Wieting, A.R., Moselle, J., Glass, C. 1988. *AIAA paper 88-0477*; also *NASP TN 1085* (1989)

Hoover, L.N., Norman, M., Cheng, H.K. 1992. (Tech. note in preparation)

Hornung, H. 1988. *Aeronautical J.* Dec.: 379-389 ; also *Z. Flugwiss. Weltraumf 12*: 293-

Hornung, H., Sturtevant B., Bélanger, J., Sanderson, S., Brouillette, M., Jenkine, M. 1992. Cal. Inst. Tech. Grad. Aero. Lab. Memo.

Hung, C.M., Barth, T.J. 1990. *AIAA J. 28: 229-235*

Hung, C.M., MacCormack, R.W. 1975. *AIAA paper 75-2*

Ito, T., Akimoto, H., Miyaba, H., Kano, Y., Suzuki, N., Sasaki, H. 1990. *AIAA paper 90-5223*

Jones, W.L., Cross, A.E. 1972. *NASA TND-6617*

Kamath, P.S., Mao., M., McClinton, C.R. 1991. *AIAA paper 91-1412*

Kang, S.W., Dunn, M.G. 1973. *NASA CR-2232*

Kang, S.W., Jones, W.L., Dunn, M.G. 1972. *AIAA J. 11*: 141-149

Kang, S.H., Kunc, J.A. 1991. *Physical Review A, 44*: 3596-3604

Kármán, Th. von, Emmons, H.W., Tankin, R.S., Taylor, G.I. 1958. *fundamental of Gas Dynamics* (ed. H.W. Emmons) Princeton Univ. Press: 574-686

Keck, J., Carrier, G. 1965. *J. Chem. Phys. 43*: 2284-2298

Kendall, J.M. 1975. *AIAA J. 13*: 240-299; see also *Aerospace Corp. Report BSD-TR-67-213,2* (1967)

Koelle, D. 1990. *AIAA paper 90-5200*

Kogan, M.N. 1969. *Rarefied Gas Dynamics* Moscow: Nauka (Transl. 1969 ed. L. Trilling, New York: Plenum)

Kogan, M.N. 1973. *Ann. Rev. Fluid Mech.*5: 383-404

Krawczyk, W., Harris, T., Rajendran, N., Carlson, D. 1989. *AIAA paper 89-1828*

Küchemann, D. 1978. *The Aerodynamic Design of Aircraft*, Pergamon Press

Kumar, A., Bushnell, D.M., Hussaini, M.Y. 1989. *J. Propulsion*: 514-522

Kunc, J.A. 1990. *J. Phys. B: At. Mol. Opt. Phys. 23*: 1-13

Kunc, J.A. 1991. *J. Phys. B: At. Mol. Opt. Phys. 24*: 3741-3761

Lam, S.H., Goussis, D.A., Konopka, D. 1989. *AIAA paper 89-0575*

Lam, S.H., Goussis, D.A. 1990. *Princeton Univ. Rept. mech. Aero. Eng. Report 1864(C)-MAE.*

Landau, L., Teller, E. 1936. *Phys. Z. Sowietunion 10*: 34-

Landrum, D., Candler, G. 1991. *AIAA paper 91-0466*

Lee, J.H. 1985. *Thermal Design of Aeroassisted Orbital Transfer Vehivles* ed. H.F. Nelson, progress of Aero. Astro. 96: 3-53

Lee, J.L. 1992. *AIAA paper 92-0807*

Lee, K.P., Gupta, R.N., Zoby, E.V., Moss, J.N. 1990. *J. Spacecraft and Rockets 27*: 185-193

Lee, R.S., Cheng, H.K. 1969. *J. Fluid Mech. 38*: 161-179

Lee, S.H., Deiwert, G.S. 1990. *J. Spacecraft and Rockets 27* : 167-174

Lee, S.L., Lin, C.C. 1946. *NACA TN 1115*

Legg, H., Koppenwallner, G. 1970. *DF-UVFL-UREV Report 70A 37a*

Lehr, H.F. 1972. *Astronautica Acta 17*: 589-597

Lesieur, M. 1990. *Turbulence in Fluids*, Klwer Acad. Publishers

Lighthill, M.J. 1953. *Proc. Roy. Soc. London A 217*: 478-

Liu, F., Jameson, A. 1992. *AIAA paper 92-0190*

Lozino-Lozinsky, Ye. G., Neiland, V. Ya. 1989. *AIAA paper 89-5019*

Lumpkin, F.E., Chapman, D.R. 1991. *AIAA paper 91-0771*, also see Lumpkin, F.E., Chapman, D.R., Park, C. 1989. *AIAA paper 89-1737*

MacCormack, R.W. 1982. *AIAA J. 20*:1275-1281

MacCormack, R.W. 1990. *AIAA paper 90-1520*

MacCormack, R.W., Baldwin, B.S. 1975, *AIAA paper 75-1*

MacCormack, R.W., Candler, G.V. 1989. *Computer and Fluid, 17* : 135-150

McDonald, J.D. 1991. *AIAA paper 91-1966*

Mack, L.M. 1984. *AGARD Report 709*; also see *AIAA J. 13*: 278-289 (1975)

Mack, L.M. 1987a *Stability of Time Dependent and Spatially Varying Flow* (ed. D.L. Dwoyer & M.Y. Hussaini), Springer, 164-187

Mack, L.M. 1987b *AIAA paper 87-1413*

Maita, M., Ohkami, Y., Yamanaka, T. 1990. *AIAA paper 90-5225*

Malik, M.R., Hussaini, M.Y. 1990. *J. Fluid Mech. 210*: 183-199

Malik, M.R., Zang, T., Bushnell, D. 1990. *AIAA paper 90-5232*

Marble, F.E., Hendricks, G.J., Zukoski, E.E. 1987. *AIAA paper 87-1880*

Marble, F.E., Zukoski, E.E., Jacobs, J.W., Hendricks, G.J., Wailz, I.A. 1990. *AIAA paper 1990-1981*

Mehta, U.B. 1990. *AIAA J. 27*: 103-112

Mikhailov, V.V., Neiland, V. Ya., Sychev, V.V. 1971. *Ann. Rev. Fluid Mechanics 3*: 371-396

Millikan, R.C., White, D.R. 1963. *J. Chem. Phys. 139*: 3209-3213

Mitcheltree, R.A. 1991. *AIAA paper 91-1368*

Moin, P. 1992. *Aerospace America* Jan.: 42-46

Moore, F.K. 1964. *Theory of Laminar Flow, Sec. E*, Princeton Univ. Press 439-527

Moss, J.N. 1976. *AIAA J. 14*: 1311-1317

Moss, J.N., Bird, G.A. 1985. *Progr. Astro. Aero. 96*: 113-139

Moss, J.N., Cuda, V., Simmonds, A.L. 1987. *AIAA paper 87-0404*

Moss, J.N., Bird, G.A., Dogra, V.K. 1988. *AIAA paper 88-0081*

Mott-Smith, H.M. 1951. *Phys. Rev. 82*: 855-

Muntz, E.P. 1989. *Ann. Rev. Fluid Mech.* 21: 387-417

Muntz, E.P., Erwin, D.A., Pham-Van-Diep, G.C. 1991. *Rarefied Gas Dynamics* (ed. A.E. Beylich), Proc. 17th Inter. Symp., Aachen, VCH Verlag, 198-206

Nelson, H.F. (ed.) 1985. *Thermal Design Aeroassisted Orbital Transfer Vehicles*, AIAA Progr. Astro. Aero. Series, *96*

Ng, L., Erlebacher, G., Zang, T.A., Pruett, D. 1990. *8th NASP Symp., Paper no. 23*

Neiland, V. Ya 1970. *Akad. Nauk. SSSR 3*: 19-

Neiland, V. Ya. 1990. (Private communication)

Nonweiler, T.R.F. 1963. *J. Roy. Aero. Soc. 67*: 39-

Nonweiler, T.R.F. 1990. *Proc. 1st Inter. Waverider Symp.*, Univ. Maryland

Nonweiler, T.R.F., Wong, H.Y., Aggarwal, S.P. 1971. *Ing. Archiv 40*:107-

Olynick, D.J., Moss, J.N., Hassan, H.A. 1990. *AIAA paper 90-1767*

Olynick, D.P., Moss, J.N., Hassan, H.A. 1991. *AIAA paper 91-1341*

Park, C. 1987. *AIAA paper 87-1574*

Park, C. 1989. *AIAA paper 89-1547*

Park, C. 1990. *Nonequilibrium Hypersonic Aerothermodynamics*, Wiley

Park, C. 1992. *AIAA paper 92-0805*

Park, C., Howe, J.T., Jaffe, R.L., Candler, G.V. 1991 *AIAA paper 91-0464*

Parker, J.G. 1959. *Phys. Fluids 2*, 449-462

Parks, S., Waldman, B. 1990. *AIAA paper 90-5229*

Parkinson, R., Conchie, P. 1990. *AIAA paper 90-5201*

Pham-Van-Diep, G.C., Erwin, D., Muntz, E.P. 1989 *Science 245*: 624-626

Pham-Van-Diep, G.C., Erwin, D., Muntz, E.P. 1991 *J Fluid Mech. 232*: 403-413

Pham-Van-Diep, G.C., Muntz, E.P., Weaver, D., Dewitt, T.G., Bradley, M.K., Erwin, D., Kunc, J 1992. *AIAA paper 92-0566*

Potter, L.J. 1988. *Progress in Aero. and Astro. 118*

Potter, L.J., Whitfield, J.D. 1965. *AGARDograph 97 pb. 3*, 1-61

Pulliam, T.H., Steger, J.L. 1980. *AIAA J. 18*: 159-167

Rapp, D., Kassal, T. 1969. *Chem. Rev. 69*: 61-

Rault, D.F.G. 1992. *AIAA paper 92-0306*

Reshotko, E. 1976. *Ann. Rev. Fluid Mech. 8*: 311-350

Reynolds, W.C. 1976. *Ann. Rev. Fluid Mech. 8*: 183-208

Rich, J.W. Treanor, C.E. 1970. *Ann. Rev. Fluid Mech. 2*: 355-396

Rizzetta, D.P., Burggaf, O.R., Jenson, R. 1978. *J. Fluid Mech. 89*:535-

Roany, A.C.G., Rich, J.W., Subramaniam, V.V., Warren, W.R. 1992. *AIAA paper 92-0252*

Roe, P.L. 1986. *Ann. Rev. Fluid Mechanics, 18*: 337-365

Rudy, D.H., Thomas, J.L., Kumar, A., Gnoffo, P.A., Chakravathy, S.R. 1991. *AIAA J. 29*: 1108-1113

Ruffin, S.M., Park, C. 1992. *AIAA paper 92-0806*

Ryan, J.S., Flores, J., Chow, C.Y. 1990. *J. Spacecraft and Rockets 27*: 160-166

Sanzero, G. 1990. *AIAA paper 90-5264*

Schwartz, R.N., Herzfeld, K.F., 1954. *J. Chem. Phys., 22*: 767-773

Schwartz, R.N., Slawsky, Z.I., Herzfeld, K.F. 1952. *J. Chem. Phys. 20*: 1591-1600

Seddougui, S.O., Bowel, R.I. and Smith, F.T. 1991. *Euro. J. Mech., B/Fluids, 10*: 117-145

Shaaf, S.A., Chambré, P.L. 1958. *Fundamentals of Gas Dynamics* ed. H.W. Emmons, Sec. H, Princeton Univ. Press: 687-739

Shang, J.S., Scherr, S.J. 1986. *J. Aircraft 23*: 881-888

Sharma, S.P., Huo, W., Park. C 1988. *AIAA paper 88-2714*

Sherman, F.S. 1969. *Ann. Rev. Fluid Mech*1: 317-340

Simon, C.E. 1976. *Theory of Shock Structure in a maxwell Gas Based on Chapman-Enskog Development through Super-Burnett Order*. Ph.D. thesis Univ. Colorado

Simen, M., Dallmann, U. 1992. *AGARD Symp. Theor. Experim. Methods Hypersonic Flows*, Torino, Italy, May 4-7, 1992

Smith, F.T. 1982. *IMA J. Appl. Math 82*: 207-

Smith, F.T. 1986. *Ann. Rev. Fluid Mech. 18*: 197-

Smith, F.T. 1989. *J. Fluid Mech. 198*: 127-153

Smith, F.T., Brown, S.N. 1990. *J. Fluid Mech. 219*: 499-518

Spall, R.E., Malik, M.R. 1989. *Phys. Fluid A, 1*: 1822-1835

Steger, J.L., Warming, R.F. 1981. *J. Comp. Phys., 40*: 263-293

Stetson, K.F. 1988. *AIAA J. 26*: 883-885

Stetson, K.F., Kimmel, R.L. 1992. *AIAA paper 92-0737*

Stewartson, K.S. 1955. *J. Aeronautical Sci. 22*: 303-309

Stewartson, K.S. 1974. *Adv. Appl. Mechanics 14*: 146-

Stewartson, K.S. 1981. *SIAM Rev. 23*: 308-

Stollery, J.L. 1990. *Proc. 1st. Inter. Hypersonic Waverider Symp.*, Univ. Maryland, College Park Md., Oct. 17-19, 1990

Stookesberry, D.C., Tannehill, J.C. 1986. *AIAA paper 86-0564*

Sutton, K. 1984. *AIAA paper 84-1733*

Sychev, V.V. 1987. *Asymptotic Theory of Separted Flows* (in Russian), Moscow Sci. Pub., Physico-Math. Literature (Distrib. USSR Nat. Comm. Theor. Appl. Mech.)

Tanczos, 1956.

Tannehill, J.C., Buelow, P.E., Levalts, J.O., Lawrence, S.L. 1990. *J. Spacecraft and Rockets, 27*: 150-159

Thomas, P.D., Neier, K.L. 1990. *J. Spacecraft & Rockets 27*: 143-149

Tirsky, G.A. 1993. *Ann. Rev. Fluid Mech. 25*: 151-181

Townend, L.H. 1991. *Phil. Trans. R. Soc. London A 335*, 201-224

Treanor, C.E. 1991. Book View *AIAA J. 29: 857-858*

Treanor, C.E., Rich, J.W., Rehm, R.G. 1968. *J. Chem. Phys. 48*: 1798-1807

van Leer, B. 1982. *Lec. Notes Phys. 170*: 507-512

van Leer, B., Thomas, J.L., Roe, P.L., Newsome, R.W 1987. *AIAA paper 87-1104-CP*

Vasta, V.N., Thomas, J.L. 1989. *J. Aircraft, 26*: 986-993

Vidal, R.J., Golian, T.C., Bartz, J.A. 1963. *AIAA paper 63-435*

Vigneron, Y.C., Rakich, J.V., Tannehill, J.C. 1978 *AIAA paper 78-1337*

Vincenti, W. G., Kruger, C.H., Jr. 1965. *Introduction to Physical Gas Dynamics*, New Yark, Wiley

Waitzel, I.A., Marble, F.E., Zukoski, E.E. 1991. *AIAA paper 91-2265*

Waitzel, I.A., Marble, F.E., Zukoski, E.E. 1992. *AIAA paper 92-0625*

Walberg, G.D. 1985. *J. Spacecraft 22 no. 1*: 30-48 (also *AIAA 82-1378*)

Waltrup, P.J., Anderson, G.Y., Stull, F.D. 1976. *Proc. 3rd Inter. Symp. Air Rreathing Engines*, 42.2-42.27

Wang-Chang, C.S. 1948. *Studies in Statistical Mechanics, V* : 27-42

Warr, J. 1970. *LMSC/HREC D 1624 98 TM 54-20-275*, Lockheed, Houston, TX.

Weiting, A. 1990. *AIAA paper 90-5238*

Werle, M.J., Dwoyer, D.L., Hankey, W.L. 1973. *AIAA J. 11*: 525-

Werle, M.J., Vasta, V.N. 1974. *AIAA J. 12*: 1491-1497

Wilcox, D.C. 1988. *AIAA J. 26*: 1299-1310

Wilcox, D.C. 1991. *AIAA paper 91-1785*

Wilke, C.R. 1950. *J. Chem. Phys. 18*: 517-

Wilhite, A.W., Airington, J.P., McCandless, R.S. 1985. *Thermal Design of Aeroassisted Orbital Transfer Vehicle* (ed. H.F. Nelson), *Progr. Astro. Aero. 96*: 165-197

Williams, F.A. 1985. *Combustion Theory: The Fundamental Theory of Chemically Reacting System*, 2nd ed. Benjamin Cummings Pub. Co. Menlo Pk. Ca.

Williams, R.M. 1986. *Aerospace American Nov.*: 18-22

Wilmoth, R.G. 1991. *AIAA paper 90-0772*; also *AIAA paper 89-1666*

Wilson, G.J., MacCormack, R.W. 1992. *AIAA J. 30*:1008-1015

Wittliff, C.E., Wilson, M.R. 1962. *ARS J. 32*: 275-276

Yang, H.T. 1992. Univ. So. Calif. Sch. Eng. Dept. Aerospace Eng. Report *USCAE 151* (in preparation)

Yee, H.C. 1987. *NASA Tech. Memo. 89464*; also *NASA Tech. Memo. 100097*

Ying, S.X., Steger, J.L., Shift, L.B., Baganoff, D. 1986. *AIAA paper 86-2179*; also see Ying, S.X. 1986. *Standford Univ. Thesis*

Yos, J.M. 1963. *AVCO-RAD Tech. memo. RAD TM-63-7*, Wilmington, Mass.

Zang, T.A., Dinavahi, S., Piomelli, U. 1989. Paper no. 26, *7th NASP Symp.*

Zhong, X., MacCormack, R.W., Chapman, D.R. 1991a. *AIAA paper 91-0770*

Zhong, X., MacCormack, R.W., Chapman, D.R. 1991b. *Proc. 4th. Inter. Symp. Comp. Fluid Dynamics*, Davis, Ca.